

Black hole tidal problem in the Fermi normal coordinates

Masaki Ishii¹, Masaru Shibata¹, and Yasushi Mino²

¹ *Graduate School of Arts and Sciences, University of Tokyo, Komaba, Meguro, Tokyo 153-8902, Japan*

² *Center for Gravitational Wave Astronomy, The University of Texas at Brownsville, 80 Fort Brown, Brownsville TX, 78520-4993 **

We derive a tidal potential for a self-gravitating fluid star orbiting Kerr black hole along a timelike geodesic extending previous works by Fishbone and Marck. In this paper, the tidal potential is calculated up to the third and fourth-order terms in R/r , where R is the stellar radius and r the orbital separation, in the Fermi-normal coordinate system following the framework developed by Manasse and Misner. The new formulation is applied for determining the tidal disruption limit (Roche limit) of corotating Newtonian stars in circular orbits moving on the equatorial plane of Kerr black holes. It is demonstrated that the third and fourth-order terms quantitatively play an important role in the Roche limit for close orbits with $R/r \gtrsim 0.1$. It is also indicated that the Roche limit of neutron stars orbiting a stellar-mass black hole near the innermost stable circular orbit may depend sensitively on the equation of state of the neutron star.

04.25.Dm, 04.25.-g, 04.40.Dg, 04.70.-s

I. INTRODUCTION

Black hole is the most compact object in the universe and can tidally disrupt ordinary stars and compact stars such as white dwarfs and neutron stars. A star of mass m and radius R will be tidally disrupted by a black hole of mass M for the case

$$\mu \equiv \frac{m}{M} \left(\frac{r}{R} \right)^3 < \mu_{\text{crit}}, \quad (1)$$

where r denotes the orbital separation and μ_{crit} is a constant ≈ 10 – 20 which depends on r/M , R/M , spin of the black hole, and equations of state (see Sec. V). If the condition (1) is satisfied outside a minimum orbital radius (e.g., $r = 6GM/c^2$ for a star in a circular orbit around a Schwarzschild black hole where c and G are the speed of light and gravitational constant), a star will be tidally disrupted. According to Eq. (1), (i) an ordinary star of mass $\sim M_\odot$ plunging inside a tidal radius of a supermassive black hole of mass smaller than $\sim 10^8 M_\odot$ will be tidally disrupted, (ii) a white dwarf of mass $\sim 0.7M_\odot$ and radius $\sim 10^4$ km plunging into a massive black hole of mass smaller than $\sim 10^5 M_\odot$ will be tidally disrupted, and (iii) an inspiraling neutron star of mass $\sim 1.4M_\odot$ and radius ~ 10 km in a circular orbit around a stellar-mass black hole of mass smaller than $\sim 5M_\odot$ will be tidally disrupted before the neutron star reaches the innermost stable circular orbit (ISCO). During the tidal interaction of the ordinary star by a supermassive black hole, an ultraviolet flare of a characteristic light-curve may be emitted at the center of galaxy and be observed (e.g., [1,2] for a review). White dwarfs or neutron stars tidally disrupted by a stellar-mass black hole will form a massive disk which may be a possible candidate of the central engine of gamma-ray bursts [3]. Detection of gravitational waves at a tidal disruption of neutron stars by a stellar-mass black hole may constrain the equation of state of neutron stars [4,5]. These examples show the tidal disruption of ordinary stars and compact objects by a black hole is likely to happen frequently and be an interesting phenomenon in the universe. This fact stimulates the theoretical study for the tidal disruption of stars by a black hole. In this paper, we present a new general relativistic formulation with higher-order corrections of the tidal potential which can be used to clarify the criterion of the tidal disruption for close orbits more accurately than that by previous works.

Numerical studies for the tidal disruption of a star by a black hole have been extensively performed assuming the Newtonian (e.g., [6–11]) or post-Newtonian [1] gravity with a point particle approximation for the black hole. However, such an approximation is not quantitatively appropriate for analyzing the tidal disruption near the black

*The present address: Mail Code 130-33, Caltech, Pasadena, CA 91125

hole, since general relativistic effects are essential for such close orbits. In [12], a numerical result for a general relativistic simulation was presented, but the authors ignored the self-gravity of the fluid star assuming that it is much weaker than the tidal force of the black hole. Relativistic tidal problems have been widely studied in the so-called tidal approximation (e.g., [13–17]). In this approximation, one assumes that the mass of a star m is much smaller than the black hole mass M and that the stellar radius R is smaller than the orbital radius r (or the curvature radius of the black hole spacetime). As a result of these assumptions, one may assume that (i) the center of mass of the star moves around the black hole along a timelike geodesic in the black hole spacetime and (ii) the tidal field from the black hole is computed from the Riemann tensor of the black hole spacetime in terms of the geodesic deviation equation. In addition to (i) and (ii), one often assumes that the self-gravity of the star is described by the Newtonian gravity. This approach has been used for studies of the tidal disruption limit of ordinary stars and compact objects [9, 11, 13, 17], and for hydrodynamic simulations of the tidal disruption of ordinary stars and white dwarfs [16]. The purpose of this paper is to improve a calculation of the tidal potential in this framework, since the improvement is necessary for some problems as explained in the following.

In the tidal approximation, one assumes $R \ll r$ and then expands the tidal potential in terms of R/r . This approximation is illustrated for the Newtonian potential ϕ as follows: Considering ϕ of a point particle of mass M_p at $(r, 0, 0)$ and expanding it around the origin, one obtains

$$\begin{aligned}\phi &= -\frac{GM_p}{\sqrt{(x-r)^2 + y^2 + z^2}} \\ &= -\frac{GM_p}{r} \left[1 + \frac{x}{r} + \frac{2x^2 - y^2 - z^2}{2r^2} + \frac{x(2x^2 - 3y^2 - 3z^2)}{2r^3} \right. \\ &\quad \left. + \frac{8x^4 - 24x^2(y^2 + z^2) + 3y^4 + 3z^4 + 6y^2z^2}{8r^4} + O(r^{-5}) \right],\end{aligned}\quad (2)$$

where we assume that $|x|, |y|, |z| \ll r$ (i.e., $R \ll r$). In the standard tidal approximation, one takes into account terms up to the second order in R/r neglecting the terms of $O[(R/r)^3]$, resulting in

$$\phi_{\text{tidal approximation}} = -\frac{GM_p}{r} \left[1 + \frac{x}{r} + \frac{2x^2 - y^2 - z^2}{2r^2} \right]. \quad (3)$$

The standard tidal approximation works for determining the tidal disruption limit in many problems, but does not in some problems: Equation (1) implies that a tidal disruption occurs if the following condition is satisfied;

$$\frac{R}{r} \gtrsim \mu_{\text{crit}}^{-1/3} Q^{1/3}. \quad (4)$$

Here, $Q \equiv m/M$. Thus, with increasing the mass ratio Q , the critical value of R/r for the tidal disruption increases: For $Q \gtrsim 10^{-3}$, the tidal disruption sets in for $R/r \gtrsim 0.05$, indicating that neglecting more than third-order terms in R/r yields an error of $\gtrsim 5\%$ and may not be a very good approximation for the computation of the tidal disruption limit. For example, the tidal disruption of white dwarfs by an intermediate mass black hole of $\sim 10^3 M_\odot$ is the case. Even for $Q < 10^{-3}$, the star will be elongated during the close-encounter with a black hole in parabolic or highly elliptical orbits. In such cases, R will increase with decreasing r , and hence, the higher-order terms may be important. For binaries of a black hole of mass smaller than $\sim 5 M_\odot$ and a neutron star in close quasicircular orbits, the higher-order terms are also important since $R/r \gtrsim 0.2$ at the ISCO of radius $\sim 6GM/c^2$. Our numerical results in the framework of Newtonian gravity indeed suggest that the third- and fourth-order terms play an important role for a system of $R/r \gtrsim 0.1$ [18]. For a rapidly rotating black hole, the radius of the ISCO can be as small as $\sim GM/c^2$. In this case, the higher-order terms in R/r may become quite important. These facts illustrate that it is often necessary to take into account the higher-order corrections of the tidal potential for computation of quantitatively improved results in the tidal problem.

In this paper, we derive a general relativistic tidal potential induced by a black hole in which higher-order corrections are taken into account. In contrast to the previous works [13, 15], we do not use the geodesic deviation equation to calculate the tidal potential. Instead, we derive the tidal metric for an observer moving along a timelike geodesic on a black hole spacetime in the Fermi normal coordinates following Manasse and Misner [19]. In this method, the tidal potential can be calculated from the tidal metric in a straightforward manner.

Using the new formulation, we numerically compute equilibrium states and a tidal disruption limit (Roche limit)[†] for corotating stars of polytropic equations of state in a close circular orbit around a Kerr black hole. Comparing the

[†]The Roche limit is defined as the tidal disruption limit for a star of corotating velocity fields.

numerical results with those computed by the standard tidal approximation, we illustrate that the higher-order terms of the tidal potential play a quantitatively important role for $R/r = O(0.1)$. The numerical results in this framework will be also used to calibrate accuracy of a numerical result of fully general relativistic quasiequilibrium states for a binary of a black hole and a neutron star which will be computed in near future. (It should be noted that there has been no comprehensive work about the tidal disruption of stars by a black hole in full general relativity, although there are primitive works for binaries of a black hole and a neutron star [21,22].) The solution obtained in this work is valid for $r \gg R$ and $M \gg m$, and hence, the calibration can be carried out for the case of low-mass neutron stars. In addition, dependence of the tidal disruption limit on the equations of state for the star is investigated. It is indicated that the tidal disruption limit of a neutron star by a stellar-mass black hole depends sensitively on the equation of state of the neutron star.

The paper is organized as follows. In Sec. II, we derive a general expression of the metric for an observer moving along timelike geodesics in the Fermi normal coordinates. In Sec. III, the results of Sec. II are applied to the Kerr spacetime. In Sec. IV, the tidal potentials are computed for equatorial circular orbits. In Sec. V, the tidal disruption limit (Roche limit) of corotating stars of equatorial circular orbits around a Kerr black hole is presented for a wide range of the spin parameter of the black hole and the equations of state for the star. Sec. VI is devoted to a summary.

In the following, we adopt the geometrical units $c = G = 1$. Latin and Greek indices denote spatial and spacetime components with $\tau = x^0$ as the time coordinate in the Fermi normal frame. $g_{\mu\nu}$, $\Gamma_{\nu\sigma}^\mu$, and $R_{\mu\nu\sigma\delta}$ denote the spacetime metric, Christoffel symbols, and Riemann tensor, respectively. $\delta_{ij}(= \delta^{ij})$ denotes the Kronecker delta. The comma and semi-colon denote the ordinary and covariant derivatives. For simplicity, we often use the notations [23]

$$A_{(ij)} = \frac{1}{2}(A_{ij} + A_{ji}), \quad (5)$$

$$A_{(ijk)} = \frac{1}{6}(A_{ijk} + A_{jik} + A_{jki} + A_{kji} + A_{kij} + A_{ikj}), \quad (6)$$

$$A_{(a_1 \dots a_l)} = \frac{1}{l!} \sum_l A_{a_{f(1)} \dots a_{f(l)}}, \quad (7)$$

where in the last equation, the sum is taken for all permutations.

II. EXTERNAL METRIC IN THE FERMI NORMAL COORDINATES

A. Outlines and definition of the Fermi normal coordinates

We derive the metric in an observer frame which moves along timelike geodesics around a Kerr black hole. As Manasse and Misner [19] show, this can be done by finding the relation between the Riemann tensor and the metric in the Fermi normal coordinate system which is one of the local inertial frames. Then, our goal is to write the metric in the neighborhood of an observer in this coordinate system as

$$g_{\mu\nu} = \eta_{\mu\nu} + \frac{1}{2}g_{\mu\nu,ij}x^i x^j + \frac{1}{6}g_{\mu\nu,ijk}x^i x^j x^k + \frac{1}{24}g_{\mu\nu,ijkl}x^i x^j x^k x^l + O(x^5), \quad (8)$$

where $\eta_{\mu\nu}$ is the flat metric and x^i denotes a spatial coordinate in the Fermi normal coordinate system. The coefficients $g_{\mu\nu,ij\dots}$ are related to the Riemann tensor of the spacetime. Using the definition of the Riemann tensor and the geodesic deviation equations, Manasse and Misner [19] derived the quadratic term in Eq. (8). Our purpose is to derive the third and fourth terms following the method developed by them.

Since the Fermi normal coordinate system is a local inertial frame, $g_{\mu\nu}$ is the flat metric along the observer frame, and the Christoffel symbols vanish

$$\Gamma_{\nu\sigma}^\mu = 0, \quad (9)$$

$$\Gamma_{\mu\nu\sigma} = g_{\mu\alpha}\Gamma_{\nu\sigma}^\alpha = 0. \quad (10)$$

In addition, the time direction in the Fermi normal coordinates is chosen as the direction of a timelike geodesic \mathcal{G} . Since Eqs. (9) and (10) are preserved along the timelike geodesic \mathcal{G} , one obtains

$$\Gamma_{\nu\sigma,0}^\mu = \Gamma_{\nu\sigma,00}^\mu = \Gamma_{\nu\sigma,0\dots 0}^\mu = 0, \quad (11)$$

$$\Gamma_{\mu\nu\sigma,0} = \Gamma_{\mu\nu\sigma,00} = \Gamma_{\mu\nu\sigma,0\dots 0} = 0. \quad (12)$$

From the definition of the Christoffel symbols,

$$g_{\mu\nu,\alpha} = \Gamma_{\mu\nu\alpha} + \Gamma_{\nu\mu\alpha}, \quad (13)$$

one finds along \mathcal{G} ,

$$g_{\mu\nu,\alpha 0} = g_{\mu\nu,\alpha 00} = g_{\mu\nu,\alpha 0 \dots 0} = 0. \quad (14)$$

B. Relation obtained from the definition of the Riemann tensor

In this subsection, we present relations necessary for deriving the tidal potential up to the fourth order using the definition of the Riemann tensor

$$R_{\mu\nu\rho\sigma} = \Gamma_{\sigma\mu\rho,\nu} - \Gamma_{\sigma\nu\rho,\mu} + \Gamma_{\nu\rho}^{\alpha}\Gamma_{\alpha\mu\sigma} - \Gamma_{\mu\rho}^{\alpha}\Gamma_{\alpha\nu\sigma}. \quad (15)$$

In the following, the components of the Riemann tensor along \mathcal{G} are computed. For $\mu = 0$ in Eq. (15), we find that the nonzero components are

$$R_{0i\nu j} = \Gamma_{j0\nu,i} = -\Gamma_{\nu 0j,i}, \quad (16)$$

where Eqs. (9)–(12) are used. For $\nu = 0$ in Eq. (16), one finds

$$g_{00,i j} = -2\Gamma_{j00,i} = -2R_{0i0j}, \quad (17)$$

where Eq. (14) is used. This gives one of the second-order terms in Eq. (8).

Since the Christoffel symbols are vanishing, the covariant derivative of the Riemann tensor is equal to the ordinary derivative along \mathcal{G} as

$$R_{\mu\nu\rho\sigma;\alpha} = R_{\mu\nu\rho\sigma,\alpha}. \quad (18)$$

Thus, from Eq. (15) and $\Gamma_{\nu\rho}^{\mu} = 0$, one obtains a relation along \mathcal{G}

$$R_{\mu\nu\rho\sigma;\alpha} = \Gamma_{\sigma\mu\rho,\nu\alpha} - \Gamma_{\sigma\nu\rho,\mu\alpha}, \quad (19)$$

and thus,

$$\begin{aligned} R_{i0j0;k} &= \Gamma_{0ij,0k} - \Gamma_{00j,ik} \\ &= \frac{1}{2} \left(g_{0i,jk} + g_{0j,ik} - g_{00,ijk} \right). \end{aligned} \quad (20)$$

Equation (20) leads to

$$R_{0i0j;k} + R_{0j0k;i} + R_{0k0i;j} = (g_{0i,jk} + g_{0j,ki} + g_{0k,ij})_{,0} - \frac{3}{2}g_{00,ijk}. \quad (21)$$

In Sec. IID, this equation is used for deriving the third-order terms in Eq. (8).

The second covariant derivative of the Riemann tensor along \mathcal{G} is written as

$$R_{\mu\nu\rho\sigma;\alpha\beta} = R_{\mu\nu\rho\sigma,\alpha\beta} - \Gamma_{\mu\beta,\alpha}^{\gamma}R_{\gamma\nu\rho\sigma} - \Gamma_{\nu\beta,\alpha}^{\gamma}R_{\mu\gamma\rho\sigma} - \Gamma_{\rho\beta,\alpha}^{\gamma}R_{\mu\nu\gamma\sigma} - \Gamma_{\sigma\beta,\alpha}^{\gamma}R_{\mu\nu\rho\gamma}. \quad (22)$$

Thus,

$$R_{\mu\nu\rho\sigma;(\alpha\beta)} = R_{\mu\nu\rho\sigma,\alpha\beta} - \Gamma_{\mu(\beta,\alpha)}^{\gamma}R_{\gamma\nu\rho\sigma} - \Gamma_{\nu(\beta,\alpha)}^{\gamma}R_{\mu\gamma\rho\sigma} - \Gamma_{\rho(\beta,\alpha)}^{\gamma}R_{\mu\nu\gamma\sigma} - \Gamma_{\sigma(\beta,\alpha)}^{\gamma}R_{\mu\nu\rho\gamma}, \quad (23)$$

and

$$R_{0i0j;(kl)} = R_{0i0j,kl} - \Gamma_{i(k,l)}^{\gamma}R_{\gamma 0j0} - \Gamma_{0(k,l)}^{\gamma}(R_{i\gamma j0} + R_{j\gamma i0}) - \Gamma_{j(k,l)}^{\gamma}R_{\gamma 0i0}. \quad (24)$$

Using Eq. (15), one obtains

$$\begin{aligned}
R_{0i0j,kl} = & \frac{1}{2} \left(g_{0i,0jkl} + g_{0j,0ikl} - g_{00,ijkl} - g_{ij,kl00} \right) \\
& + \Gamma_{0i,k}^\alpha \Gamma_{\alpha 0j,l} + \Gamma_{0i,l}^\alpha \Gamma_{\alpha 0j,k} - \Gamma_{00,l}^\alpha \Gamma_{\alpha ij,k} - \Gamma_{00,k}^\alpha \Gamma_{\alpha ij,l},
\end{aligned} \tag{25}$$

and hence,

$$\begin{aligned}
& R_{0i0j,kl} + R_{0i0k,jl} + R_{0i0l,jk} + R_{0j0k,il} + R_{0j0l,ik} + R_{0k0l,ij} \\
= & \frac{3}{2} (g_{0i,jkl} + g_{0j,ikl} + g_{0k,ijl} + g_{0l,ijk})_{,0} - 3g_{00,ijkl} \\
& - \frac{1}{2} (g_{ij,kl} + g_{ik,jl} + g_{il,jk} + g_{jk,il} + g_{jl,ik} + g_{kl,ij})_{,00} \\
& + 4(\Gamma_{0(i,j)}^\alpha \Gamma_{\alpha 0(k,l)} + \Gamma_{0(i,k)}^\alpha \Gamma_{\alpha 0(j,l)} + \Gamma_{0(i,l)}^\alpha \Gamma_{\alpha 0(j,k)}) \\
& - 3(\Gamma_{00,i}^\alpha \Gamma_{\alpha(jk,l)} + \Gamma_{00,j}^\alpha \Gamma_{\alpha(ik,l)} + \Gamma_{00,k}^\alpha \Gamma_{\alpha(ij,l)} + \Gamma_{00,l}^\alpha \Gamma_{\alpha(ij,k)}).
\end{aligned} \tag{26}$$

In Sec. IID, this equation is used to derive the fourth-order terms in Eq. (8).

C. Relations obtained from the geodesic deviation equations

In this subsection, relations necessary for calculating the tidal potential up to the fourth order are derived using the geodesic deviation equations.

For the tangent of a geodesic, u^μ , and the displacement vector to an infinitesimally nearby geodesic z^μ , the geodesic deviation equation is written as

$$u^\mu \nabla_\mu (u^\nu \nabla_\nu z^\sigma) = -R_{\mu\nu\gamma}{}^\sigma u^\mu u^\gamma z^\nu. \tag{27}$$

Note here that the geodesic that we consider is not restricted to \mathcal{G} . Using an affine parameter λ for the geodesic (i.e., $u^\mu = (\partial/\partial\lambda)^\mu$), Eq. (27) is rewritten to

$$\frac{d^2 z^\mu}{d\lambda^2} + 2 \frac{dz^\nu}{d\lambda} \Gamma_{\nu\sigma}^\mu u^\sigma + (\Gamma_{\nu\alpha,\sigma}^\mu + \Gamma_{\nu\beta}^\mu \Gamma_{\alpha\sigma}^\beta - \Gamma_{\alpha\beta}^\mu \Gamma_{\nu\sigma}^\beta) u^\nu u^\sigma z^\alpha = -R_{\nu\alpha\sigma}{}^\mu u^\nu u^\sigma z^\alpha, \tag{28}$$

or

$$\frac{d^2 z^\mu}{d\lambda^2} + 2 \frac{dz^\nu}{d\lambda} \Gamma_{\nu\sigma}^\mu u^\sigma + \Gamma_{\nu\sigma,\alpha}^\mu u^\nu u^\sigma z^\alpha = 0. \tag{29}$$

Now, we consider the family of spacelike geodesics in the Fermi normal coordinates of the form

$$x^0 = \text{const.} \quad \text{and} \quad x^i = \alpha^i \lambda, \tag{30}$$

where α^i is a constant three-component. Using its definition, u^μ is written to

$$u^\mu = \left(\frac{\partial}{\partial\lambda} \right)^\mu = \delta_i^\mu \alpha^i. \tag{31}$$

As the displacement vector z^σ , we choose the spatial vector defined by

$$z^\mu = \left(\frac{\partial}{\partial\alpha^i} \right)^\mu = \lambda \delta_i^\mu. \tag{32}$$

Substituting Eqs. (31) and (32) into Eq. (29) leads to

$$2\Gamma_{ij}^\mu \alpha^j + \lambda \Gamma_{jk,i}^\mu \alpha^j \alpha^k = 0. \tag{33}$$

Our purpose here is to derive the relations among the derivatives of the Christoffel symbols along \mathcal{G} which will be useful in the subsequent calculations. To obtain the relations, Eq. (33) should be evaluated for $\lambda = 0$. However, Eq. (33) is trivial because of the vanishing Christoffel symbols in the Fermi normal coordinates. Thus, we carry out a Taylor expansion of Eq. (33) assuming that λ is small, and the first-, second-, and third-order terms in λ provide

$$2\Gamma_{ij,k}^\mu \alpha^j \alpha^k + \Gamma_{jk,i}^\mu \alpha^j \alpha^k = 0, \quad (34)$$

$$\Gamma_{ij,kl}^\mu \alpha^j \alpha^k \alpha^l + \Gamma_{jk,il}^\mu \alpha^j \alpha^k \alpha^l = 0, \quad (35)$$

$$\frac{1}{3}\Gamma_{ij,kl n}^\mu \alpha^j \alpha^k \alpha^l \alpha^n + \frac{1}{2}\Gamma_{jk,il n}^\mu \alpha^j \alpha^k \alpha^l \alpha^n = 0. \quad (36)$$

Equations (34)–(36) lead to cyclic relations among the derivatives of the Christoffel symbols along \mathcal{G} as

$$\Gamma_{\mu(ij,k)} = 0, \quad (37)$$

$$\Gamma_{\mu(ij,kl)} = 0, \quad (38)$$

$$\Gamma_{\mu(ij,kl n)} = 0. \quad (39)$$

Setting $\mu = 0$ in Eqs. (37)–(39), the following useful relations are derived;

$$g_{0(i,jk)} = 0, \quad (40)$$

$$3(g_{0i,jkl} + g_{0j,ikl} + g_{0k,ijl} + g_{0l,ijk}) = (g_{ij,kl} + g_{ik,jl} + g_{il,jk} + g_{jk,il} + g_{jl,ik} + g_{kl,ij}),_0, \quad (41)$$

$$4(g_{0i,jkln} + g_{0j,ikln} + g_{0k,ijln} + g_{0l,ijkn} + g_{0n,ijkl}) \\ = (g_{ij,kl n} + g_{ik,jl n} + g_{il,jk n} + g_{in,jkl} + g_{jk,il n} + g_{jl,ik n} + g_{jn,ikl} + g_{kl,ijn} + g_{kn,ijl} + g_{ln,ijk}),_0. \quad (42)$$

Using Eq. (28) with the same strategy as that for deriving Eqs. (34)–(36), one can also obtain relations among the Christoffel symbols and Riemann tensor as

$$R_{ijk}{}^\mu \alpha^j \alpha^k = 3\Gamma_{ij,k}^\mu \alpha^j \alpha^k, \quad (43)$$

$$R_{ijk}{}^\mu{}_{,l} \alpha^j \alpha^k \alpha^l = 2\Gamma_{ij,kl}^\mu \alpha^j \alpha^k \alpha^l, \quad (44)$$

$$\frac{1}{2}R_{ijk}{}^\mu{}_{,ln} \alpha^j \alpha^k \alpha^l \alpha^n = \frac{5}{6}\Gamma_{ij,kl n}^\mu \alpha^j \alpha^k \alpha^l \alpha^n + (\Gamma_{ij,l}^\sigma \Gamma_{\sigma k,n}^\mu - \Gamma_{i\sigma,l}^\mu \Gamma_{jk,n}^\sigma) \alpha^j \alpha^k \alpha^l \alpha^n. \quad (45)$$

Here, $\Gamma_{jk,n}^\sigma \alpha^j \alpha^k \alpha^n = 0$ because of Eq. (37). Thus, the last term of Eq. (45) vanishes.

From Eqs. (43)–(45) together with Eqs. (37)–(39), one obtains the relations between the Christoffel symbols and the Riemann tensor along \mathcal{G} as

$$\Gamma_{ij,k}^\mu + \Gamma_{ik,j}^\mu = -\frac{1}{3}\left(R_{jik}{}^\mu + R_{kij}{}^\mu\right), \quad (46)$$

$$\Gamma_{ij,kl}^\mu + \Gamma_{ik,jl}^\mu + \Gamma_{il,jk}^\mu = -\frac{1}{4}\left(R_{jik}{}^\mu{}_{,l} + R_{jil}{}^\mu{}_{,k} + R_{kij}{}^\mu{}_{,l} + R_{lij}{}^\mu{}_{,k} + R_{lik}{}^\mu{}_{,j} + R_{kil}{}^\mu{}_{,j}\right), \quad (47)$$

$$\Gamma_{ij,kl n}^\mu + \Gamma_{ik,jl n}^\mu + \Gamma_{il,jk n}^\mu + \Gamma_{in,jkl}^\mu \\ = \frac{2}{5}\left(R_{i(jk)}{}^\mu{}_{,ln} + R_{i(jl)}{}^\mu{}_{,kn} + R_{i(jn)}{}^\mu{}_{,kl} + R_{i(kl)}{}^\mu{}_{,jn} + R_{i(kn)}{}^\mu{}_{,jl} + R_{i(ln)}{}^\mu{}_{,jk}\right) \\ - \frac{4}{5}\left(\Gamma_{i(j,k)}^\nu \Gamma_{\nu(l,n)}^\mu + \Gamma_{i(j,l)}^\nu \Gamma_{\nu(k,n)}^\mu + \Gamma_{i(j,n)}^\nu \Gamma_{\nu(k,l)}^\mu + \Gamma_{i(k,l)}^\nu \Gamma_{\nu(j,n)}^\mu + \Gamma_{i(k,n)}^\nu \Gamma_{\nu(j,l)}^\mu + \Gamma_{i(l,n)}^\nu \Gamma_{\nu(j,k)}^\mu\right) \quad (48)$$

Using Eq. (37), Eq. (46) is rewritten to

$$\Gamma_{\mu jk,i} = -\frac{2}{3}R_{i(jk)\mu}. \quad (49)$$

For $\mu = 0$ in Eq. (49),

$$-\frac{2}{3}R_{i(jk)0} = \Gamma_{0jk,i} = \frac{1}{2}(g_{0j,ik} + g_{0k,ij}) = -\frac{1}{2}g_{0i,jk}, \quad (50)$$

where Eqs. (40) and $g_{jk,i0} = 0$ are used. Thus,

$$g_{0k,ij} = \frac{2}{3}\left(R_{0ijk} + R_{0jik}\right). \quad (51)$$

This gives one of the second-order terms in Eq. (8).

Equation (49) is also used to derive the relation for $g_{kl,ij}$ along \mathcal{G}

$$g_{kl,ij} = \Gamma_{kli,j} + \Gamma_{lki,j} = \frac{1}{3} \left(R_{iklj} + R_{iljk} \right). \quad (52)$$

This also gives one of the second-order terms in Eq. (8).

From Eqs. (52), one finds the following relations along \mathcal{G} ;

$$g_{i(j,kl)} = 0, \quad (53)$$

$$g_{(kl,j)i} = 0. \quad (54)$$

Equations (40), (53), and (54) are preserved along \mathcal{G} , i.e.,

$$[g_{0(k,ij)},_0] = 0, \quad (55)$$

$$[g_{i(j,kl)},_0] = 0, \quad (56)$$

$$[g_{(kl,j)i},_0] = 0. \quad (57)$$

Substituting the last two relations into Eq. (41), one obtains

$$g_{0(i,jkl)} = 0. \quad (58)$$

These relations are useful for deriving the third-order terms in Eq. (8).

D. Deriving the third- and fourth-order terms

From Eqs. (21), (40), (47), (55), and (58), third derivatives of 00 and 0i components of the metric are found to be

$$g_{00,ijk} = -\frac{2}{3} \left(R_{0i0j;k} + R_{0j0k;i} + R_{0k0i;j} \right) = -2R_{0(i|0|j;k)}, \quad (59)$$

$$g_{0i,jkl} = \frac{1}{4} \left(R_{ijk0;l} + R_{ikj0;l} + R_{ilk0;j} + R_{ikl0;j} + R_{ijl0;k} + R_{ilj0;k} \right) = \frac{3}{2} R_{i(jk|0|l)}. \quad (60)$$

For ij components,

$$\begin{aligned} g_{ij,kl n} &= \Gamma_{ijk,ln} + \Gamma_{jik,ln} \\ &= \frac{1}{3} \left(\Gamma_{ijk,ln} + \Gamma_{jil,kn} + \Gamma_{ijn,kl} + \Gamma_{jik,ln} + \Gamma_{jil,kn} + \Gamma_{jin,kl} \right) \\ &= -\frac{1}{6} \left(R_{kjl i;n} + R_{kjni;l} + R_{ljki;n} + R_{njki;l} + R_{njli;k} + R_{ljni;k} \right), \end{aligned} \quad (61)$$

where we use Eqs. (38) and (47).

Using Eqs. (24), (26), and (41), the fourth derivative of 00 component of the metric is written as

$$\begin{aligned} g_{00,ijkl} &= -\frac{1}{3} \left[R_{0i0j;(kl)} + R_{0i0k;(jl)} + R_{0i0l;(jk)} + R_{0j0k;(il)} + R_{0j0l;(ik)} + R_{0k0l;(ij)} \right] \\ &\quad + \frac{8}{3} \left[\Gamma_{0(k,l)}^\mu \Gamma_{\mu 0(i,j)} + \Gamma_{0(j,l)}^\mu \Gamma_{\mu 0(i,k)} + \Gamma_{0(i,l)}^\mu \Gamma_{\mu 0(j,k)} \right] \\ &= -\frac{1}{3} \left[R_{0i0j;(kl)} + R_{0i0k;(jl)} + R_{0i0l;(jk)} + R_{0j0k;(il)} + R_{0j0l;(ik)} + R_{0k0l;(ij)} \right] \\ &\quad + \frac{8}{3} \left[R_{(kl)0}^\mu R_{\mu(ij)0} + R_{(jl)0}^\mu R_{\mu(ik)0} + R_{(jk)0}^\mu R_{\mu(il)0} \right] \\ &= -2R_{0(i|0|j;kl)} + 8R_{(kl|0|}^\mu R_{|\mu|ij)0}. \end{aligned} \quad (62)$$

From Eq. (61) and $R_{(ijk)l} = 0$, it is found

$$g_{(ij,kl)n} = g_{i(j,kl)n} = 0, \quad (63)$$

and hence,

$$[g_{(ij,kl)n}]_{,0} = [g_{i(j,kl)n}]_{,0} = 0. \quad (64)$$

Using Eqs. (64) and (42), one obtains

$$g_{0(i,jkl)n} = 0. \quad (65)$$

By a straightforward calculation, one finds

$$\Gamma_{\mu ij,kl n} + \Gamma_{\mu ik,jl n} + \Gamma_{\mu il,jk n} + \Gamma_{\mu in,jkl} = 2[g_{\mu i,jkl n} + g_{\mu(j,kl)n i} - g_{i(j,kl)n \mu}]. \quad (66)$$

For $\mu = 0$ in Eq. (66),

$$\Gamma_{0ij,kl n} + \Gamma_{0ik,jl n} + \Gamma_{0il,jk n} + \Gamma_{0in,jkl} = \frac{3}{2}g_{0i,jkl n}, \quad (67)$$

where Eqs. (63) and (65) are used. Thus,

$$\begin{aligned} g_{0i,jkl n} &= \frac{2}{3} \left(\Gamma_{0ij,kl n} + \Gamma_{0ik,jl n} + \Gamma_{0il,jk n} + \Gamma_{0in,jkl} \right) \\ &= \frac{4}{15} \left(R_{i(jk)0,ln} + R_{i(jl)0,kn} + R_{i(jn)0,kl} + R_{i(kl)0,jn} + R_{i(kn)0,jl} + R_{i(ln)0,jk} \right) \\ &\quad - \frac{8}{15} \left(\Gamma_{i(j,k)}^\nu \Gamma_{0\nu(l,n)} + \Gamma_{i(j,l)}^\nu \Gamma_{0\nu(k,n)} + \Gamma_{i(j,n)}^\nu \Gamma_{0\nu(k,l)} \right. \\ &\quad \left. + \Gamma_{i(k,l)}^\nu \Gamma_{0\nu(j,n)} + \Gamma_{i(k,n)}^\nu \Gamma_{0\nu(j,l)} + \Gamma_{i(l,n)}^\nu \Gamma_{0\nu(j,k)} \right) \\ &= \frac{4}{15} \left(R_{i(jk)0,ln} + R_{i(jl)0,kn} + R_{i(jn)0,kl} + R_{i(kl)0,jn} + R_{i(kn)0,jl} + R_{i(ln)0,jk} \right) \\ &\quad - \frac{8}{45} \left(R_{i(jk)}^0 R_{0(ln)0} + R_{i(jl)}^0 R_{0(kn)0} + R_{i(jn)}^0 R_{0(kl)0} + R_{i(kl)}^0 R_{0(jn)0} + R_{i(kn)}^0 R_{0(jl)0} + R_{i(ln)}^0 R_{0(jk)0} \right) \\ &\quad - \frac{8}{135} \left(R_{i(jk)}^m R_{m(ln)0} + R_{i(jl)}^m R_{m(kn)0} + R_{i(jn)}^m R_{m(kl)0} \right. \\ &\quad \left. + R_{i(kl)}^m R_{m(jn)0} + R_{i(kn)}^m R_{m(jl)0} + R_{i(ln)}^m R_{m(jk)0} \right) \\ &= \frac{8}{5} R_{i(jk|0|,ln)} - \frac{16}{15} R_{i(jk)}^0 R_{0|ln)0} - \frac{16}{45} R_{i(jk)}^m R_{m|ln)0}, \end{aligned} \quad (68)$$

where we use Eq. (48).

The fourth derivative of ij components is derived as follows:

$$\begin{aligned} g_{ij,klmn} &= \Gamma_{ijk,lmn} + \Gamma_{jik,lmn} \\ &= \frac{1}{5} \left[R_{i(kl)j,mn} + R_{i(km)j,ln} + R_{i(kn)j,lm} + R_{i(lm)j,kn} + R_{i(ln)j,km} + R_{i(mn)j,kl} \right] \\ &\quad - \frac{1}{5} \left[\Gamma_{i(k,l)}^\nu \Gamma_{j\nu(m,n)} + \Gamma_{i(k,m)}^\nu \Gamma_{j\nu(l,n)} + \Gamma_{i(k,n)}^\nu \Gamma_{j\nu(l,m)} \right. \\ &\quad \left. + \Gamma_{i(l,m)}^\nu \Gamma_{j\nu(k,n)} + \Gamma_{i(l,n)}^\nu \Gamma_{j\nu(k,m)} + \Gamma_{i(m,n)}^\nu \Gamma_{j\nu(k,l)} \right. \\ &\quad \left. + \Gamma_{j(k,l)}^\nu \Gamma_{i\nu(m,n)} + \Gamma_{j(k,m)}^\nu \Gamma_{i\nu(l,n)} + \Gamma_{j(k,n)}^\nu \Gamma_{i\nu(l,m)} \right. \\ &\quad \left. + \Gamma_{j(l,m)}^\nu \Gamma_{i\nu(k,n)} + \Gamma_{j(l,n)}^\nu \Gamma_{i\nu(k,m)} + \Gamma_{j(m,n)}^\nu \Gamma_{i\nu(k,l)} \right] \\ &= \frac{1}{5} \left[R_{i(kl)j,mn} + R_{i(km)j,ln} + R_{i(kn)j,lm} + R_{i(lm)j,kn} + R_{i(ln)j,km} + R_{i(mn)j,kl} \right] \end{aligned}$$

	00 components	equation	0i components	equation	ij components	equation
2nd order	$g_{00,ij}$	(17)	$g_{0i,jk}$	(51)	$g_{ij,kl}$	(52)
3rd order	$g_{00,ijk}$	(59)	$g_{0i,jkl}$	(60)	$g_{ij,klm}$	(61)
4th order	$g_{00,ijkl}$	(62)	$g_{0i,jklm}$	(68)	$g_{ij,klmn}$	(69)

TABLE I. Equation numbers from which one finds the relation between $g_{\mu\nu,ijk\dots}$ and the corresponding Riemann tensor in the Fermi normal coordinates.

$$\begin{aligned}
& -\frac{2}{15} \left[R_{i(kl)}{}^0 R_{j(mn)0} + R_{i(km)}{}^0 R_{j(ln)0} + R_{i(kn)}{}^0 R_{j(lm)0} \right. \\
& \quad \left. + R_{i(lm)}{}^0 R_{j(kn)0} + R_{i(ln)}{}^0 R_{j(km)0} + R_{i(mn)}{}^0 R_{j(kl)0} \right] \\
& -\frac{2}{45} \left[R_{i(kl)}{}^p R_{j(mn)p} + R_{i(km)}{}^p R_{j(ln)p} + R_{i(kn)}{}^p R_{j(lm)p} \right. \\
& \quad \left. + R_{i(lm)}{}^p R_{j(kn)p} + R_{i(ln)}{}^p R_{j(km)p} + R_{i(mn)}{}^p R_{j(kl)p} \right] \\
& = \frac{6}{5} R_{i(kl|j|,mn)} - \frac{4}{5} R_{i(kl)}{}^0 R_{j|mn)0} - \frac{4}{15} R_{i(kl)}{}^p R_{j|mn)p}.
\end{aligned} \tag{69}$$

We note that the second ordinary derivatives of the Riemann tensor in Eqs. (68) and (69) are transformed to the covariant derivatives using

$$R_{i(jk|0|;ln)} = R_{i(jk|0|,ln)} - \frac{4}{3} R_{i(nl)}{}^\sigma R_{|\sigma|jk)0}, \tag{70}$$

$$R_{i(jk|m|;ln)} = R_{i(jk|m|,ln)} - \frac{2}{3} R_{i(nl)}{}^\sigma R_{|\sigma|jk)m}. \tag{71}$$

This implies that $g_{0i,jklm}$ and $g_{ij,klmn}$ can be written in the covariant form.

To summarize this section, we derive the coefficients $g_{\mu\nu,ijk\dots}$ in Eq. (8) which denotes the metric at $\tau = x^0 = \text{constant}$ in the neighborhood of the timelike geodesic \mathcal{G} . This is used as the tidal field from a black hole for a star moving along \mathcal{G} . The equation numbers for the relations between the derivatives of the metric and the Riemann tensor in the Fermi normal coordinates are summarized in Table I.

III. COMPONENTS OF THE RIEMANN TENSOR FOR A KERR SPACETIME

To compute components of the Riemann tensor and its covariant derivative for the Kerr metric in the Fermi normal coordinates, we adopt the method developed by Marck [15]. Namely, we first calculate the components in a standard tetrad frame of the Boyer-Lindquist coordinate system [24], and then, perform a coordinate transformation to the Fermi normal coordinates.

The Kerr metric in the Boyer-Lindquist coordinate system is written as

$$ds^2 = -\left(1 - \frac{2Mr}{\Sigma}\right) dt^2 - \frac{4Mra \sin^2 \theta}{\Sigma} dt d\varphi + \frac{(r^2 + a^2)^2 - \Delta a^2 \sin^2 \theta}{\Sigma} \sin^2 \theta d\varphi^2 + \frac{\Sigma}{\Delta} dr^2 + \Sigma d\theta^2, \tag{72}$$

where

$$\Sigma = r^2 + a^2 \cos^2 \theta, \quad \Delta = r^2 + a^2 - 2Mr, \tag{73}$$

and M and a denote the mass and spin parameter. A standard tetrad for the Kerr metric is defined by

$$(e^{(0)})_\mu = \left(\sqrt{\frac{\Delta}{\Sigma}}, 0, 0, -a \sin^2 \theta \sqrt{\frac{\Delta}{\Sigma}} \right), \tag{74}$$

$$(e^{(1)})_\mu = \left(0, \sqrt{\frac{\Sigma}{\Delta}}, 0, 0 \right), \tag{75}$$

$$(e^{(2)})_\mu = (0, 0, \sqrt{\Sigma}, 0), \quad (76)$$

$$(e^{(3)})_\mu = \left(-\frac{a \sin \theta}{\sqrt{\Sigma}}, 0, 0, \frac{(r^2 + a^2) \sin \theta}{\sqrt{\Sigma}} \right). \quad (77)$$

Note that the sign convention for $(e^{(3)})_\mu$ is different from that of [15].

In the first step, we compute the components of the Riemann tensor and its covariant derivative in the standard tetrad. The nonvanishing components of the Riemann tensor in this tetrad frame are

$$\begin{aligned} R_{(1)(2)(1)(2)} &= R_{(1)(3)(1)(3)} = \frac{1}{2}R_{(1)(0)(1)(0)} = -\frac{1}{2}R_{(2)(3)(2)(3)} \\ &= -R_{(2)(0)(2)(0)} = -R_{(3)(0)(3)(0)} = \frac{Mr(3a^2 \cos^2 \theta - r^2)}{\Sigma^3}, \end{aligned} \quad (78)$$

$$R_{(1)(2)(3)(0)} = -R_{(1)(3)(2)(0)} = -\frac{1}{2}R_{(1)(0)(2)(3)} = \frac{aM \cos \theta (3r^2 - a^2 \cos^2 \theta)}{\Sigma^3}. \quad (79)$$

The tetrad components associated with the first and second covariant derivatives are defined as

$$Q_{(a)(b)(c)(d)(e)} \equiv \nabla_\mu R_{\nu\rho\sigma\lambda} (e_{(a)})^\mu (e_{(b)})^\nu (e_{(c)})^\rho (e_{(d)})^\sigma (e_{(e)})^\lambda, \quad (80)$$

$$P_{(a)(b)(c)(d)(e)(f)} \equiv \nabla_{(\alpha} \nabla_{\beta)} R_{\nu\rho\sigma\lambda} (e_{(a)})^\alpha (e_{(b)})^\beta (e_{(c)})^\nu (e_{(d)})^\rho (e_{(e)})^\sigma (e_{(f)})^\lambda. \quad (81)$$

The nonvanishing components of $Q_{(a)(b)(c)(d)(e)}$ are

$$\begin{aligned} Q_{(a)(1)(2)(1)(2)} &= Q_{(a)(1)(3)(1)(3)} = \frac{1}{2}Q_{(a)(1)(0)(1)(0)} = -\frac{1}{2}Q_{(a)(2)(3)(2)(3)} = -Q_{(a)(2)(0)(2)(0)} = -Q_{(a)(3)(0)(3)(0)} \\ &= \left(\frac{3MJ_1 \Delta^{1/2}}{\Sigma^{9/2}}, -\frac{12Ma^2 r J_2 \sin \theta \cos \theta}{\Sigma^{9/2}}, 0, 0 \right), \end{aligned} \quad (82)$$

$$Q_{(a)(1)(2)(1)(0)} = Q_{(a)(2)(3)(3)(0)} = \left(0, 0, \frac{-12MarJ_2 \Delta^{1/2} \cos \theta}{\Sigma^{9/2}}, -\frac{12Ma^2 r J_2 \sin \theta \cos \theta}{\Sigma^{9/2}} \right), \quad (83)$$

$$Q_{(a)(1)(2)(2)(3)} = -Q_{(a)(1)(0)(3)(0)} = \left(0, 0, \frac{3MJ_1 \Delta^{1/2}}{\Sigma^{9/2}}, \frac{3MaJ_1 \sin \theta}{\Sigma^{9/2}} \right), \quad (84)$$

$$Q_{(a)(1)(2)(3)(0)} = -Q_{(a)(1)(3)(2)(0)} = -\frac{1}{2}Q_{(a)(1)(0)(2)(3)} = \left(-\frac{12Mar \Delta^{1/2} J_2 \cos \theta}{\Sigma^{9/2}}, -\frac{3MaJ_1 \sin \theta}{\Sigma^{9/2}}, 0, 0 \right), \quad (85)$$

$$Q_{(a)(1)(3)(1)(0)} = -Q_{(a)(2)(3)(2)(0)} = \left(-\frac{3MaJ_1 \sin \theta}{\Sigma^{9/2}}, \frac{12MarJ_2 \Delta^{1/2} \cos \theta}{\Sigma^{9/2}}, 0, 0 \right), \quad (86)$$

$$Q_{(a)(1)(3)(2)(3)} = Q_{(a)(1)(0)(2)(0)} = \left(-\frac{12Ma^2 r J_2 \sin \theta \cos \theta}{\Sigma^{9/2}}, -\frac{3MJ_1 \Delta^{1/2}}{\Sigma^{9/2}}, 0, 0 \right), \quad (87)$$

where

$$J_1 = r^4 - 6a^2 r^2 \cos^2 \theta + a^4 \cos^4 \theta, \quad (88)$$

$$J_2 = r^2 - a^2 \cos^2 \theta. \quad (89)$$

For $P_{(a)(b)(c)(d)(e)(f)}$, the explicit form of the components in a general orbit is very complicated. Thus, we only write the nonvanishing components in the equatorial plane setting $\theta = \pi/2$;

$$P_{(a)(b)(1)(2)(1)(2)} = -P_{(a)(b)(3)(0)(3)(0)} = \frac{3M}{r^7} \begin{pmatrix} -(4r^2 - 9rM + 5a^2) & 0 & 0 & 0 \\ * & \Delta + 4a^2 & 0 & 0 \\ * & * & 3\Delta & 3a\Delta^{1/2} \\ * & * & * & -(Mr - 3a^2) \end{pmatrix}, \quad (90)$$

$$P_{(a)(b)(1)(2)(1)(3)} = P_{(a)(b)(2)(0)(3)(0)} = -\frac{3M}{r^7} \begin{pmatrix} 0 & 0 & 0 & 0 \\ * & 0 & \Delta & a\Delta^{1/2} \\ * & * & 0 & 0 \\ * & * & * & 0 \end{pmatrix}, \quad (91)$$

$$P_{(a)(b)(1)(2)(1)(0)} = P_{(a)(b)(2)(3)(3)(0)} = \frac{3M}{2r^7} \begin{pmatrix} 0 & 0 & 0 & 0 \\ * & 0 & 8a\Delta^{1/2} & -(Mr - 8a^2) \\ * & * & 0 & 0 \\ * & * & * & 0 \end{pmatrix}, \quad (92)$$

$$P_{(a)(b)(1)(2)(2)(3)} = -P_{(a)(b)(1)(0)(3)(0)} = -\frac{3M}{2r^7} \begin{pmatrix} 0 & 0 & 8\Delta - Mr & 8a\Delta^{1/2} \\ * & 0 & 0 & 0 \\ * & * & 0 & 0 \\ * & * & * & 0 \end{pmatrix}, \quad (93)$$

$$P_{(a)(b)(1)(2)(2)(0)} = -P_{(a)(b)(1)(3)(3)(0)} = \frac{3M}{r^7} \begin{pmatrix} 0 & 0 & a\Delta^{1/2} & a^2 \\ * & 0 & 0 & 0 \\ * & * & 0 & 0 \\ * & * & * & 0 \end{pmatrix}, \quad (94)$$

$$\frac{1}{15}P_{(a)(b)(1)(2)(3)(0)} = -\frac{1}{21}P_{(a)(b)(1)(3)(2)(0)} = -\frac{1}{36}P_{(a)(b)(1)(0)(2)(3)} = \frac{M}{r^7} \begin{pmatrix} 0 & a\Delta^{1/2} & 0 & 0 \\ * & 0 & 0 & 0 \\ * & * & 0 & 0 \\ * & * & * & 0 \end{pmatrix}, \quad (95)$$

$$P_{(a)(b)(1)(3)(1)(3)} = -P_{(a)(b)(2)(0)(2)(0)} = \frac{3M}{r^7} \begin{pmatrix} -(4r^2 - 9Mr + 7a^2) & 0 & 0 & 0 \\ * & (3\Delta + 4a^2) & 0 & 0 \\ * & * & \Delta & a\Delta^{1/2} \\ * & * & * & -Mr + a^2 \end{pmatrix}, \quad (96)$$

$$P_{(a)(b)(1)(3)(1)(0)} = -P_{(a)(b)(2)(3)(2)(0)} = \frac{3M}{2r^7} \begin{pmatrix} 16a\Delta^{1/2} & 0 & 0 & 0 \\ * & -16a\Delta^{1/2} & 0 & 0 \\ * & * & 0 & -Mr \\ * & * & * & 0 \end{pmatrix}, \quad (97)$$

$$P_{(a)(b)(1)(3)(2)(3)} = P_{(a)(b)(1)(0)(2)(0)} = \frac{3M}{2r^7} \begin{pmatrix} 0 & 8r^2 - 17Mr + 16a^2 & 0 & 0 \\ * & 0 & 0 & 0 \\ * & * & 0 & 0 \\ * & * & * & 0 \end{pmatrix}, \quad (98)$$

$$P_{(a)(b)(1)(0)(1)(0)} = -P_{(a)(b)(2)(3)(2)(3)} = \frac{6M}{r^7} \begin{pmatrix} -(4r^2 - 9Mr + 6a^2) & 0 & 0 & 0 \\ * & 2(\Delta + 2a^2) & 0 & 0 \\ * & * & 2\Delta & 2a\Delta^{1/2} \\ * & * & * & -(Mr - 2a^2) \end{pmatrix}. \quad (99)$$

Here, the components in the 2-matrix form of the subscripts (a) and (b) are shown in the order (1), (2), (3), and (0).

To compute R_{abcd} , Q_{abcde} , and P_{abcdef} in the Fermi normal coordinates, we need to prepare the transformation matrix from the standard tetrad frame to the Fermi normal coordinate frame. Denoting it as $\Lambda_a^{(a)}$, we have

$$R_{abcd} = R_{(a)(b)(c)(d)} \Lambda_a^{(a)} \Lambda_b^{(b)} \Lambda_c^{(c)} \Lambda_d^{(d)}, \quad (100)$$

$$Q_{abcde} = Q_{(a)(b)(c)(d)(e)} \Lambda_a^{(a)} \Lambda_b^{(b)} \Lambda_c^{(c)} \Lambda_d^{(d)} \Lambda_e^{(e)}, \quad (101)$$

$$P_{abcdef} = P_{(a)(b)(c)(d)(e)(f)} \Lambda_a^{(a)} \Lambda_b^{(b)} \Lambda_c^{(c)} \Lambda_d^{(d)} \Lambda_e^{(e)} \Lambda_f^{(f)}. \quad (102)$$

$\Lambda_a^{(a)}$ is constructed from an orthonormal set of vectors λ_a^μ ($a = 0, 1, 2, 3$), which are parallel-propagated along a timelike geodesic \mathcal{G} as

$$\Lambda_a^{(a)} = \lambda_a^\mu (e^{(a)})_\mu. \quad (103)$$

Since the tangent vector of the timelike geodesic, $u^\mu \equiv (\partial/\partial\tau)^\mu$, is parallel-propagated along \mathcal{G} , λ_0^μ should be equal to u^μ . Here, the geodesic equations are integrated to give (e.g., [15])

$$u^t = \frac{1}{\Delta\Sigma} [(r^2 + a^2)\Sigma E - 2MarB], \quad (104)$$

$$(\Sigma u^r)^2 = A^2 - \Delta(r^2 + K), \quad (105)$$

$$(\Sigma u^\theta)^2 = K - a^2 \cos^2 \theta - \frac{B^2}{\sin^2 \theta}, \quad (106)$$

$$u^\varphi = \frac{1}{\Delta \Sigma \sin^2 \theta} [-2MrB + L\Sigma], \quad (107)$$

where

$$A = E(r^2 + a^2) - aL, \quad B = L - aE \sin^2 \theta. \quad (108)$$

$E = -u_t$ and $L = u_\varphi$ are the specific energy and angular momentum for a particle of mass μ moving around a Kerr black hole. $K = (L - aE)^2 + C_K$ is the so-called Carter constant with C_K a constant [25]. The first integral of the geodesic equations leads to

$$\Lambda_0^{(0)} = \frac{A}{\sqrt{\Delta \Sigma}}, \quad (109)$$

$$\Lambda_0^{(1)} = \frac{\sqrt{\Sigma} u^r}{\sqrt{\Delta}}, \quad (110)$$

$$\Lambda_0^{(2)} = \sqrt{\Sigma} u^\theta, \quad (111)$$

$$\Lambda_0^{(3)} = \frac{B}{\sqrt{\Sigma} \sin \theta}. \quad (112)$$

For other components of $\lambda_a^{(a)}$, we follow Marck [15], and thus, we choose

$$\Lambda_1^{(0)} = \frac{\alpha \sqrt{\Sigma} r u^r}{\sqrt{K \Delta}} \cos \Psi - \frac{\alpha A}{\sqrt{\Delta \Sigma}} \sin \Psi, \quad (113)$$

$$\Lambda_1^{(1)} = \frac{\alpha r A}{\sqrt{K \Delta \Sigma}} \cos \Psi - \frac{\alpha \sqrt{\Sigma} u^r}{\sqrt{\Delta}} \sin \Psi, \quad (114)$$

$$\Lambda_1^{(2)} = -\frac{\beta a B \cos \theta}{\sqrt{K \Sigma} \sin \theta} \cos \Psi - \beta \sqrt{\Sigma} u^\theta \sin \Psi, \quad (115)$$

$$\Lambda_1^{(3)} = \frac{\beta \sqrt{\Sigma} a u^\theta \cos \theta}{\sqrt{K}} \cos \Psi - \frac{\beta B}{\sqrt{\Sigma} \sin \theta} \sin \Psi, \quad (116)$$

$$\Lambda_2^{(0)} = \frac{\sqrt{\Sigma} a \cos \theta u^r}{\sqrt{K \Delta}}, \quad (117)$$

$$\Lambda_2^{(1)} = \frac{a A \cos \theta}{\sqrt{K \Delta \Sigma}}, \quad (118)$$

$$\Lambda_2^{(2)} = \frac{r B}{\sqrt{K \Sigma} \sin \theta}, \quad (119)$$

$$\Lambda_2^{(3)} = -\frac{\sqrt{\Sigma} r u^\theta}{\sqrt{K}}, \quad (120)$$

$$\Lambda_3^{(0)} = \frac{\alpha \sqrt{\Sigma} r u^r}{\sqrt{K \Delta}} \sin \Psi + \frac{\alpha A}{\sqrt{\Delta \Sigma}} \cos \Psi, \quad (121)$$

$$\Lambda_3^{(1)} = \frac{\alpha r A}{\sqrt{K \Delta \Sigma}} \sin \Psi + \frac{\alpha \sqrt{\Sigma} u^r}{\sqrt{\Delta}} \cos \Psi, \quad (122)$$

$$\Lambda_3^{(2)} = -\frac{\beta a B \cos \theta}{\sqrt{K \Sigma} \sin \theta} \sin \Psi + \beta \sqrt{\Sigma} u^\theta \cos \Psi, \quad (123)$$

$$\Lambda_3^{(3)} = \frac{\beta \sqrt{\Sigma} a u^\theta \cos \theta}{\sqrt{K}} \sin \Psi + \frac{\beta B}{\sqrt{\Sigma} \sin \theta} \cos \Psi, \quad (124)$$

where α and β are normalization constants defined by

$$\alpha = \sqrt{\frac{K - a^2 \cos^2 \theta}{r^2 + K}}, \quad \beta = \frac{1}{\alpha}. \quad (125)$$

We note that the direction of the components 1, 2, and 3 [not (1), (2), and (3)] adopted by Marck are approximately equal to x , $-z$, and y of the Cartesian coordinates in the comoving frame. The time evolution of the rotation angle Ψ is computed by

$$\frac{d\Psi}{d\tau} = \frac{\sqrt{K}}{\Sigma} \left(\frac{A}{r^2 + K} + \frac{aB}{K - a^2 \cos^2 \theta} \right). \quad (126)$$

IV. FORMULATION FOR EQUILIBRIUM NEWTONIAN STARS IN EQUATORIAL CIRCULAR ORBITS IN THE BLACK HOLE TIDAL FIELD

A. Basic equations

In this section, we give a formulation for computing equilibrium states of a fluid star in circular orbits around equatorial plane of a Kerr spacetime. Here, we assume that the self-gravity of the star is described by the Newtonian gravity. In this case, the gravitational potential associated with the tidal potential can be linearly superposed [13]. Using this property, we write the hydrodynamic equation for the fluid body as

$$\rho \frac{\partial v_i}{\partial \tau} + \rho v^j \frac{\partial v_i}{\partial x^j} = -\frac{\partial P}{\partial x^i} - \rho \frac{\partial(\phi + \phi_{\text{tidal}})}{\partial x^i} + \rho \left[v_j \left(\frac{\partial A_j}{\partial x^i} - \frac{\partial A_i}{\partial x^j} \right) - \frac{\partial A_i}{\partial \tau} \right], \quad (127)$$

where ρ is the mass density, v^i the three-velocity ($dx^i/d\tau$), P the pressure, and ϕ the Newtonian potential produced by a star which obeys the Poisson equation

$$\Delta\phi = 4\pi\rho. \quad (128)$$

A_i is a vector potential defined in Eq.(134), which is associated with the so-called gravitomagnetic force [26]. ϕ_{tidal} denotes the tidal potential associated with the background Kerr spacetime, which is related to the metric computed in previous sections as

$$\begin{aligned} \phi_{\text{tidal}} &= -\frac{1}{2}(g_{00} + 1) \\ &= -\frac{1}{4}g_{00,ij}x^i x^j - \frac{1}{12}g_{00,ijk}x^i x^j x^k - \frac{1}{48}g_{00,ijkl}x^i x^j x^k x^l + O(x^5) \\ &= \frac{1}{2}C_{ij}x^i x^j + \frac{1}{6}C_{ijk}x^i x^j x^k + \frac{1}{24}[C_{ijkl} + 4C_{(ij}C_{kl)} - 4B_{(kl|n|}B_{ij)n}]x^i x^j x^k x^l + O(x^5), \end{aligned} \quad (129)$$

where

$$C_{ij} = R_{0i0j}, \quad (130)$$

$$C_{ijk} = R_{0(i0|j;k)}, \quad (131)$$

$$C_{ijkl} = R_{0(i0|j;k;l)}, \quad (132)$$

$$B_{ijk} = R_{k(ij)0}, \quad (133)$$

$$A_k = \frac{2}{3}B_{ijk}x^i x^j. \quad (134)$$

In the equations of motion (127), we include the lowest-order gravitomagnetic term associated with A_k , although it is a first post-Newtonian term and does not appear in Newtonian order from the point of view of post-Newtonian approximations [27]. The reason we add it is that the order of magnitude of this term is as large as that of the fourth-order terms in ϕ_{tidal} if the spin angular velocity of the fluid star is of order Ω as in the corotational velocity field (see a discussion in the final paragraph of this section). On the other hand, for the irrotational velocity field in which the spin of the fluid star is negligible in the frame of the Fermi normal coordinates, the magnitude of this term will be much smaller than the fourth-order term in ϕ_{tidal} . In the following calculation, we neglect the gravitomagnetic terms for most of calculations, but to clarify the quantitative effect of this term, we perform a few computations including it.

In this paper, we restrict our attention to circular orbits in the equatorial plane, i.e., $\theta = \pi/2$, $u^r = 0$, $u^\theta = 0$, and $C_K = 0$. Then [20]

$$E = \frac{r^2 - 2Mr + a\sqrt{Mr}}{rD}, \quad (135)$$

$$L = \frac{\sqrt{Mr}(r^2 - 2a\sqrt{Mr} + a^2)}{rD}, \quad (136)$$

$$D \equiv \sqrt{r^2 - 3Mr + 2a\sqrt{Mr}}, \quad (137)$$

where r denotes the orbital radius. In this case, the evolution equation for Ψ becomes

$$\frac{d\Psi}{d\tau} = \sqrt{\frac{M}{r^3}}, \text{ and hence, } \Psi = \sqrt{\frac{M}{r^3}}\tau. \quad (138)$$

For the equatorial circular orbits, the transformation matrix $\Lambda_a^{(a)}$ reduces to a simple form as

$$\Lambda_0^{(a)} = \left(\sqrt{1 + \frac{B^2}{r^2}}, 0, 0, \frac{B}{r} \right), \quad (139)$$

$$\Lambda_1^{(a)} = \left(-\frac{B}{r} \sin \Psi, \cos \Psi, 0, -\sqrt{1 + \frac{B^2}{r^2}} \sin \Psi \right), \quad (140)$$

$$\Lambda_2^{(a)} = (0, 0, 1, 0), \quad (141)$$

$$\Lambda_3^{(a)} = \left(\frac{B}{r} \cos \Psi, \sin \Psi, 0, \sqrt{1 + \frac{B^2}{r^2}} \cos \Psi \right), \quad (142)$$

where $B = L - aE = r(\sqrt{Mr} - a)/D$. Note that $1 + B^2/r^2$ may be written as Δ/D^2 . A known interesting property is that independent of the value of a , $B/r = 1/\sqrt{3}$ and $\Delta/D = 4/3$ at ISCOs [13] at which r satisfies

$$r^2 - 6Mr + 8M^{1/2}ar^{1/2} - 3a^2 = 0. \quad (143)$$

This implies that at the ISCO, $r^3 C_{ij}$ and $r^3 B_{ijk}$ are independent of a (see below).

To derive the tidal tensors C_{ij} , C_{ijk} , C_{ijkl} , and B_{ijk} , as a first step, it is better to calculate the components in a tetrad frame defined by

$$\tilde{\Lambda}_0^{(a)} = \Lambda_0^{(a)}, \quad (144)$$

$$\tilde{\Lambda}_1^{(a)} = \Lambda_1^{(a)} \cos \Psi + \Lambda_3^{(a)} \sin \Psi, \quad (145)$$

$$\tilde{\Lambda}_2^{(a)} = \Lambda_2^{(a)}, \quad (146)$$

$$\tilde{\Lambda}_3^{(a)} = -\Lambda_1^{(a)} \sin \Psi + \Lambda_3^{(a)} \cos \Psi. \quad (147)$$

We refer to this frame as the tilde frame in the following. In the tilde frame, $\tilde{\Lambda}_a^{(a)}$ is independent of Ψ , but the coordinate basis of this frame is not parallel-transported along the timelike geodesic. In the second step, we should perform the coordinate transformation to the parallel-transported frame.

The nonvanishing components of \tilde{C}_{ij} , \tilde{C}_{ijk} , \tilde{C}_{ijkl} , and \tilde{B}_{ijk} , which denote the tidal tensor in the tilde frame, are

$$\tilde{C}_{11} = \frac{M}{r^3} \left(1 - 3 \frac{r^2 + B^2}{r^2} \right), \quad (148)$$

$$\tilde{C}_{22} = \frac{M}{r^3} \left(1 + 3 \frac{B^2}{r^2} \right), \quad (149)$$

$$\tilde{C}_{33} = \frac{M}{r^3}, \quad (150)$$

$$\tilde{B}_{131} = \tilde{B}_{311} = -\tilde{B}_{232} = -\tilde{B}_{322} = -\frac{1}{2} \tilde{B}_{113} = \frac{1}{2} \tilde{B}_{223} = -\frac{3MB}{2r^4} \sqrt{1 + \frac{B^2}{r^2}}, \quad (151)$$

$$\tilde{C}_{111} = \frac{3M\Delta^{1/2}}{Dr^7} [2Dr^2 - 2aBr + 3B^2D], \quad (152)$$

$$\tilde{C}_{122} = \tilde{C}_{212} = \tilde{C}_{221} = -\frac{M\Delta^{1/2}}{Dr^7} [3Dr^2 - 8aBr + 7B^2D], \quad (153)$$

$$\tilde{C}_{133} = \tilde{C}_{313} = \tilde{C}_{331} = -\frac{M\Delta^{1/2}}{Dr^7} [3Dr^2 + 2aBr + 2B^2D], \quad (154)$$

$$\tilde{C}_{1111} = \frac{3M}{Dr^9} [-8Dr^4 + 18DMr^3 + 16aBr\Delta - 12(a^2 + B^2)Dr^2 + 27B^2DMr - 19a^2B^2D], \quad (155)$$

$$\begin{aligned} \tilde{C}_{1122} &= \tilde{C}_{1212} = \tilde{C}_{1221} = \tilde{C}_{2112} = \tilde{C}_{2121} = \tilde{C}_{2211} \\ &= \frac{M}{2Dr^9} [24Dr^4 - 51DMr^3 - 108aBr\Delta + 51(a^2 + B^2)Dr^2 - 109B^2DMr + 102a^2B^2D], \end{aligned} \quad (156)$$

$$\begin{aligned}\tilde{C}_{1133} &= \tilde{C}_{1313} = \tilde{C}_{1331} = \tilde{C}_{3113} = \tilde{C}_{3131} = \tilde{C}_{3311} \\ &= \frac{M}{2Dr^{11}} [24Dr^6 - 51DMr^5 + 20aBr^3\Delta + 25(a^2 + B^2)Dr^4 - 56B^2DMr^3 \\ &\quad + 10aB^3r\Delta + 5B^4Dr^2 + 25a^2B^2Dr^2 - 15B^4DMr + 10a^2B^4D],\end{aligned}\quad (157)$$

$$\tilde{C}_{2222} = -\frac{3M}{Dr^9} [3Dr^4 - 6DMr^3 - 16aBr\Delta + 7(a^2 + B^2)Dr^2 - 14B^2DMr + 19a^2B^2D], \quad (158)$$

$$\begin{aligned}\tilde{C}_{2233} &= \tilde{C}_{2323} = \tilde{C}_{2332} = \tilde{C}_{3223} = \tilde{C}_{3232} = \tilde{C}_{3322} \\ &= \frac{M}{2Dr^{11}} [-6Dr^6 + 12DMr^5 + 10aBr^3\Delta - 10(a^2 + B^2)Dr^4 + 21B^2DMr^3 \\ &\quad - 10aB^3r\Delta - 5B^4Dr^2 + 5a^2B^2Dr^2 + 15B^4DMr - 10a^2B^4D],\end{aligned}\quad (159)$$

$$\tilde{C}_{3333} = \frac{3M}{Dr^9} [-3Dr^4 + 6DMr^3 - 6aBr\Delta - 3(a^2 + B^2)Dr^2 + 7B^2DMr - 6a^2B^2D]. \quad (160)$$

The expression for \tilde{C}_{ij} agrees with that derived by Marck [15]. The nonvanishing components of C_{ij} , C_{ijk} , C_{ijkl} , and B_{ijk} are derived by the coordinate transformation from \tilde{x}^i to x^i .

In the tilde frame, the tidal potential up to the fourth order is written as

$$\phi_{\text{tidal}} = \frac{1}{2}\tilde{C}_{ij}\tilde{x}^i\tilde{x}^j + \frac{1}{6}\tilde{C}_{ijk}\tilde{x}^i\tilde{x}^j\tilde{x}^k + \frac{1}{24}[\tilde{C}_{ijkl} + 4\tilde{C}_{(ij}\tilde{C}_{kl)} - 4\tilde{B}_{(kl|n|}\tilde{B}_{ij)n}]\tilde{x}^i\tilde{x}^j\tilde{x}^k\tilde{x}^l, \quad (161)$$

where

$$\tilde{x}^1 = x^1 \cos \Psi + x^3 \sin \Psi, \quad (162)$$

$$\tilde{x}^2 = x^2, \quad (163)$$

$$\tilde{x}^3 = -x^1 \sin \Psi + x^3 \cos \Psi. \quad (164)$$

In the Newtonian limit $r \gg M(> a)$, it is written as

$$\begin{aligned}\phi_{\text{tidal}} &= \frac{M}{2r^3} [-2(\tilde{x}^1)^2 + (\tilde{x}^2)^2 + (\tilde{x}^3)^2] - \frac{M}{2r^4} \tilde{x}^1 [-2(\tilde{x}^1)^2 + 3\{(\tilde{x}^2)^2 + (\tilde{x}^3)^2\}] \\ &\quad - \frac{M}{8r^5} [8(\tilde{x}^1)^4 + 3(\tilde{x}^2)^4 + 3(\tilde{x}^3)^4 - 24\{(\tilde{x}^1)^2(\tilde{x}^2)^2 + (\tilde{x}^1)^2(\tilde{x}^3)^2\} + 6(\tilde{x}^2)^2(\tilde{x}^3)^2].\end{aligned}\quad (165)$$

This agrees with the expansion form of the Newtonian tidal potential from a point source of mass M at a distance r as

$$- \frac{M}{\sqrt{(\tilde{x}^1 + r)^2 + (\tilde{x}^2)^2 + (\tilde{x}^3)^2}}. \quad (166)$$

The orders of the magnitude of the second-, third-, and fourth-order tidal forces in Eq. (165) are $O(MR/r^3)$, $O(MR^2/r^4)$, and $O(MR^3/r^5)$, respectively. On the other hand, the order of magnitude of the gravitomagnetic force in the Fermi normal coordinates is $O(M^{3/2}Rv/r^{7/2})$ where v denotes the characteristic magnitude of v^i . For the corotational velocity field, $v = O(M^{1/2}R/r^{3/2})$, and hence, the gravitomagnetic tidal force is of $O(M^2R^2/r^5)$ which is the same as the order of the fourth-order tidal potential for stars with $R = O(M)$. For close corotating orbits with $r = O(M)$, it is as large as the third-order term. For rapidly rotating stars with $v \lesssim c$, the gravitomagnetic tidal force is always larger than the third-order term. On the other hand, for the irrotational velocity field, it will be negligible.

B. Hydrostatic equations for corotational and irrotational equilibria

Now, we turn our attention to the hydrostatic equations. First, we consider the case in which the velocity field is corotational, and assume

$$v^i = [-\{x^3 - x_c \sin(\Omega\tau)\}, 0, \{x^1 - x_c \cos(\Omega\tau)\}] \quad (167)$$

where $\Omega = d\Psi/d\tau = \text{const.}$ x_c is a correction constant which is much smaller than the stellar radius and nonzero only when we take into account the third-order terms in ϕ_{tidal} or the gravitomagnetic terms. For $x_c \neq 0$, the rotational axis deviates from the x^2 axis. Also, the center of mass of a fluid star is different from the origin slightly (see Sec. V).

In this velocity field, Eq. (127) is integrated to give

$$\frac{\Omega^2}{2}[(\tilde{x}^1 - x_g)^2 + (\tilde{x}^3)^2] = h + \phi + \phi_{\text{tidal}} + \phi_{\text{mag}} + C, \quad (168)$$

where $x_g = 2x_c$, C is an integration constant, and

$$h = \int \frac{dP}{\rho}, \quad (169)$$

$$\phi_{\text{mag}} = 2\frac{MB}{r^4}\sqrt{1 + \frac{B^2}{r^2}}\Omega\left[-(\tilde{x}^1)^3 + \tilde{x}^1\{(\tilde{x}^2)^2 - (\tilde{x}^3)^2\} + \frac{3}{4}x_g\{(\tilde{x}^1)^2 - (\tilde{x}^2)^2\}\right]. \quad (170)$$

The first integral of the Euler equation is independent of τ in the tilde frame. Equations (128) and (168) constitute the basic equations for the corotational binary.

For the irrotational velocity field, we should set the three-components of the four-velocity as

$$u_i \equiv v_i + A_i = \frac{\partial\psi}{\partial x^i}, \quad (171)$$

where ψ denotes the velocity potential which is time-independent in the tilde frame. Then, Eq. (127) is integrated to give

$$-\frac{\partial\psi}{\partial\tau} - \frac{1}{2}\delta_{ij}\frac{\partial\psi}{\partial x^i}\frac{\partial\psi}{\partial x^j} = h + \phi + \phi_{\text{tidal}} - \frac{\partial\psi}{\partial x^j}A^j + C. \quad (172)$$

In the tilde frame, the first term is written as

$$-\frac{\partial\psi}{\partial\tau} = \Omega\tilde{x}^i\frac{\partial\psi}{\partial\tilde{x}^i}. \quad (173)$$

Also, we have a relation

$$\delta_{ij}\frac{\partial\psi}{\partial x^i}\frac{\partial\psi}{\partial x^j} = \delta_{ij}\frac{\partial\psi}{\partial\tilde{x}^i}\frac{\partial\psi}{\partial\tilde{x}^j}. \quad (174)$$

Thus, the first integral of the Euler equation is also independent of τ in the tilde frame.

ψ is determined by solving the continuity equation rewritten as

$$\rho\tilde{\Delta}\psi + \delta_{ij}\frac{\partial\psi}{\partial\tilde{x}^i}\frac{\partial\rho}{\partial\tilde{x}^j} = 0, \quad (175)$$

where $\tilde{\Delta}$ is the Laplacian in the tilde coordinates. Equations (128), (172), and (175) constitute the basic equations for irrotational binaries.

V. ROCHE LIMIT IN EQUATORIAL CIRCULAR ORBITS

To quantitatively illustrate the importance of the higher-order terms in the tidal potential ϕ_{tidal} as well as to clarify the dependence of the tidal disruption limit of a star on the equations of state and on general relativistic effects of the black hole, we numerically compute corotating equilibria and determine the tidal disruption limit (Roche limit) as an extension of a previous work by Fishbone [13]. For some case such as binaries of a black hole and a neutron star, the irrotational velocity field is more realistic. However, we know that in the incompressible case, the tidal disruption limit depends weakly on the velocity profile as far as the spin angular velocity of the star is of order $M^{1/2}/r^{3/2}$ [17]. We expect that this will be also the case for compressible stars, and hence, even in the assumption of the corotational velocity field, we can obtain an approximate result of the tidal disruption limit for the irrotational velocity field.

A. Setting and numerical method

We adopt polytropic equations of state for the star as

$$P = \kappa \rho^{1+\frac{1}{n}}, \text{ and thus, } h = \kappa(n+1)\rho^{\frac{1}{n}}, \quad (176)$$

where κ is the polytropic constant and n the polytropic index. In this paper, we choose $n = 0.5, 1$, and 1.5 to approximately model neutron stars or white dwarfs.

The basic equations in this problem are Eqs. (128) and (168). Numerical solutions are obtained by iteratively solving these coupled equations. To achieve a convergence in the iteration, we rescale the coordinates as $\tilde{x}^i = pq^i$ where p is a constant and q^i dimensionless coordinates. Then, the basic equations are written in the form

$$\Delta_q \bar{\phi} = 4\pi\rho, \quad (177)$$

$$\frac{\Omega^2}{2} p^2 [(\bar{q}^1 - q_g)^2 + (\bar{q}^3)^2] = h + p^2 \bar{\phi} + p^2 (\bar{\phi}_{\text{tidal}} + \bar{\phi}_{\text{mag}}) + C, \quad (178)$$

where Δ_q is the Laplacian in the coordinates of q^i , $\bar{\phi} = p^{-2}\phi$, $\bar{\phi}_{\text{tidal}} = p^{-2}\phi_{\text{tidal}}$, $\bar{\phi}_{\text{mag}} = p^{-2}\phi_{\text{mag}}$, and $q_g = q^{-2}x_g$. Thus, six free constants M , a , κ , q_g , p , and C are contained in the equations. In the following, M is fixed adopting the units $c = G = M = 1$. An equilibrium configuration is computed for fixed values of κ , ρ_c (the central density), a , and $r(> R)$. Sequences of the equilibria are computed varying these parameters. κ and ρ_c determine the mass m and the radius R of a star, and so do the ratios $Q = m/M$ and R/r . Note that for a given value of r , Ω is determined to be $(M/r^3)^{1/2}$ in this problem.

Three remained constants q_g , p , and C are parameters determined at each step of the iteration from the following conditions: During the iteration, we require that $\rho = \rho_c$ and $\partial\rho/\partial q^1 = 0$ at the origin $(q^1, q^2, q^3) = (0, 0, 0)$. In addition, we fix the coordinates of the stellar surface along the \tilde{x}^1 axis (the axis connecting the origin and the center of a black hole) on the black hole side as $(q_s, 0, 0)$ where $q_s < 0$. From these three conditions, the three free parameters are determined.

If we include the third-order terms in the tidal potential, the center of mass of a star may be deviated from the origin, although for consistency, it should be located approximately there. To check that the deviation is much smaller than the stellar radius, we calculate the value of q^1 coordinate for a center of mass defined by

$$\langle q^1 \rangle \equiv \frac{p^3}{m} \int d^3q \rho q^1, \quad (179)$$

where

$$m \equiv p^3 \int d^3q \rho. \quad (180)$$

We found that $|\langle q^1 \rangle|$ is indeed much smaller than the stellar radius (e.g., $|\langle q^1 \rangle| \sim 0.005|q_s|$ at ISCOs for $a = 0-0.9M$ and the value is smaller for smaller orbital radii).

The Poisson equation (177) is solved in the Cartesian coordinates with the uniform grid of size $(2N+1, N+1, 2N+1)$ for (q^1, q^2, q^3) which covers the region with $-L \leq q^1 \leq L$, $0 \leq q^2 \leq L$, and $-L \leq q^3 \leq L$ (the reflection symmetry with respect to the $q^2 = 0$ plane is assumed). The numerical method is essentially the same as that in [28]: We make the second-order finite-differencing equation and solve it in a preconditioned conjugate gradient method. Typically, N and the grid spacing Δ are set to be 50 and $|q_s|/40$. To check the convergence, we varied the values of $(N, |q_s|/\Delta)$ as (60, 48), (50, 30), and (40, 32). It is found that the numerical results converge at the second order and the error is within 0.1% with (50, 40).

Following Fishbone [13], we often refer to a nondimensional parameter defined by

$$\zeta \equiv \frac{\Omega^2}{\pi\rho_c} = \frac{M}{\pi\rho_c r^3}. \quad (181)$$

The order of magnitude of this parameter is

$$\zeta \sim \frac{MR^3}{mr^3} = \frac{MR/r^3}{m/R^2}. \quad (182)$$

Thus, it denotes the ratio of the tidal force by a black hole to the self-gravity of a star. In particular, we focus on the value of ζ at the Roche limit, which is denoted by ζ_{crit} in the following. ζ_{crit} is a function of r/M and depends on

the equations of state and the black hole spin. We can also compute the minimum allowed mass of a star that can escape tidal disruption for a given radius. The critical mass ratio associated with such minimum mass is defined by $Q_{\text{crit}} = (m/M)_{\text{minimum}}$. Q_{crit} is also a function of r and depends on the equations of state and the black hole spin. A star will be tidally disrupted for $Q < Q_{\text{crit}}$.

Numerical computations for determining ζ_{crit} and Q_{crit} are performed approximately fixing the value of an averaged stellar radius for a given set of r , a , and n . The stellar radius of a spherical polytrope R_0 is written by [29]

$$R_0 = \left[\frac{(n+1)\kappa\rho_c^{(1-n)/n}}{4\pi} \right]^{1/2} \xi_1 = \left(\frac{h_c}{4\pi\rho_c} \right)^{1/2} \xi_1, \quad (183)$$

where $h_c = \kappa(n+1)\rho_c$ and ξ_1 denotes the Lane-Emden coordinate at the stellar surface, which is 2.75270, π , and 3.65375 for $n = 0.5$, 1, and 1.5, respectively. Note that for $n = 1$, fixing the value of κ is equivalent to fixing the value of R_0 . For other values of n , κ varies along a sequence of a fixed value of R_0 .

To determine the Roche limit for a given set of r , a , and n , we compute a sequence of solutions by varying ρ_c from a large value to a small value until an inner edge of the star forms a cusp on the black hole side. A configuration with such a cusp can be identified as the Roche limit, i.e., the self-gravity of the star is small enough to form a saddle point of the total gravitational potential at a stellar surface. Specifically, the Roche limit is determined monitoring the following quantity at $(q^1, q^2, q^3) = (q_s, 0, 0)$:

$$H \equiv \Omega^2(q_s - q_g) - \frac{\partial(\bar{\phi} + \bar{\phi}_{\text{tidal}})}{\partial q^1}. \quad (184)$$

Here, H is proportional to $\partial h / \partial q^1$. Thus, the value of H for $q_s < 0$ is positive for stable stars, and becomes zero for the marginally stable configuration against tidal disruption.

In this paper, we are in particular interested in making approximate models of binaries composed of a stellar-mass black hole of mass $M \sim 3\text{--}30M_\odot$ and a neutron star of mass $m \sim 1.4M_\odot$. It is appropriate to assume that the radius of neutron stars is between 10 and 15 km. Then, R_0 in the present units should be between $\sim 3M$ and $\sim 0.2M$. In the following calculation, we adopt the values of R_0/M as 0.5, 1, and 2. For consistency in the framework of this paper, (i) R_0 should be much smaller than r , (ii) m should be much smaller than M , and (iii) r should be larger than the orbital radius of an ISCO (hereafter r_{ISCO}) around the black hole. Thus, the computations are performed only for $m < M$ and for $r \geq r_{\text{ISCO}}$. It would not be quantitatively appropriate to model a neutron star by Newtonian gravity since neutron stars are compact with $m/R_0 \sim 0.2$ and thus general relativistic objects. The following numerical results could contain a systematic error of magnitude $\sim m/R_0$. However, the quantitative importance of the higher-order terms as well as the general relativistic effects in the tidal potential can be clarified even if we neglect the general relativistic corrections of neutron stars. Also, the present study will be useful for qualitatively clarifying the dependence of the Roche limit on the equations of state.

B. Tidal potential

In Fig. 1, we display the tidal potential ϕ_{tidal} along \tilde{x}^1 , \tilde{x}^2 , and \tilde{x}^3 axes. Figures 1(a)–(c) show ϕ_{tidal} for $(r/M, a/M) = (6, 0)$, $(2, 1)$, and $(6, 1)$, respectively. Figure 1(d) is ϕ_{tidal} in the fourth-order approximation for $a = M$ and $r/M = 1.2, 1.5, 2$, and 3. To clarify the convergence with increasing the order, ϕ_{tidal} in the second- (dotted-dashed curves), third- (dashed curves), and fourth-order (solid curves) approximations are shown together in Figs. 1(a)–(c). ϕ_{tidal} in the second- and third-order approximations are identical along \tilde{x}^2 and \tilde{x}^3 axes. Thus, only the second-order results are presented. At the second order, ϕ_{tidal} is symmetric with respect to the origin along all the axial directions. The third-order terms induce an asymmetry in the \tilde{x}^1 direction.

The difference in the magnitude of ϕ_{tidal} is about 20–30% between the second- and fourth-order approximations for $|\tilde{x}^i| \sim R_0 \sim M$ near the ISCOs. For $|\tilde{x}^i| \lesssim R_0 \sim M$, the difference in the magnitude of the third- and fourth-order tidal potentials is $\lesssim 1\%$, and hence, the convergence is approximately achieved. ϕ_{tidal} in the third- and fourth-order approximations are larger than that in the second-order approximation in the black hole side ($\tilde{x}^1 < 0$). This indicates that a star becomes prone to tidal disruption in the higher-order approximations.

Comparing Figs. 1(a) and (c) for which the results with the same value of r are shown, it is found that the spin effect reduces the magnitude of ϕ_{tidal} along \tilde{x}^1 and \tilde{x}^2 axes. This illustrates the property that for the larger value of a/M , the tidal effect is weaker for a given value of r/M . Figure 1(d) shows that the magnitude of $r^3\phi_{\text{tidal}}$ in the black hole side is smaller for the smaller values of r . This suggests that a star is less prone to the tidal disruption for an extremely high value of $a \approx M$ near the ISCOs. Such a special feature is not outstanding for other values of a .

C. Roche limits

In Fig. 2, we show ζ_{crit} and $\mu_{\text{crit}} \equiv Q_{\text{crit}}(r/R_0)^3$ as functions of r/M (a) for $n = 1$, $a = 0$, and $R_0/M = 0, 0.5, 1$, and 2, and (b) for $n = 1$, $a = 0.9M$, and $R_0/M = 0, 0.5$ and 1. Stars with $\zeta < \zeta_{\text{crit}}$ and $\mu > \mu_{\text{crit}}$ for a given value of r/M are stable against tidal disruption. The computations for $R_0 \neq 0$ were performed taking into account the tidal potential up to fourth order. Note that the values of ζ_{crit} and μ_{crit} in the third- and fourth-order approximations with $R_0 = 0$ are equal to those in the second-order approximation with an arbitrary value of R_0 . Thus, “ $R_0 = 0$ ” implies that the computations were performed in the second-order tidal approximation. With increasing R_0/M , ζ_{crit} (μ_{crit}) at a given orbital radius decreases (increases). This illustrates that the tidal force in the fourth-order approximation is stronger than in the second-order one.

As in previous works [13,17] carried out by the second-order tidal approximation, ζ_{crit} (μ_{crit}) decreases (increases) with decreasing r/M . This implies that with the decrease of r/M , the tidal force is enhanced. At $r = r_{\text{ISCO}}$, ζ_{crit} and μ_{crit} become minimum and maximum for given values of a and R_0 . We denote them by $\zeta_{\text{crit:min}}$ and $\mu_{\text{crit:max}}$. On the other hand, for $r \rightarrow \infty$, ζ_{crit} and μ_{crit} become maximum and minimum for given values of a and R_0 , and they agree with the values in the Newtonian limit [18]. For given values of a and R_0 , a star at an ISCO has to be tidally disrupted whenever $\zeta > \zeta_{\text{crit}} \geq \zeta_{\text{crit:min}}$ or $\mu < \mu_{\text{crit}} \leq \mu_{\text{crit:max}}$. In other words, for $\zeta < \zeta_{\text{crit:min}}$ and $\mu > \mu_{\text{crit:max}}$, the star in a circular orbit is not tidally disrupted outside the ISCOs.

In Figs. 2(c) and (d), $\zeta_{\text{crit}}/\zeta_{\text{crit:2nd}} - 1$ and $\mu_{\text{crit}}/\mu_{\text{crit:2nd}} - 1$ as functions of M/r are shown for the same parameters as in Figs. 2(a) and (b), respectively. Here, $\zeta_{\text{crit:2nd}}$ and $\mu_{\text{crit:2nd}}$ denote ζ_{crit} and μ_{crit} determined in the second-order tidal approximation. We note that in the second-order tidal approximation, ζ_{crit} and μ_{crit} are independent of R_0 . It is found that for $M/r (\lesssim 0.1)$, $\zeta_{\text{crit}}/\zeta_{\text{crit:2nd}} - 1$ and $\mu_{\text{crit}}/\mu_{\text{crit:2nd}} - 1$ are approximately linear functions of M/r . Thus, for the large values of r/M , the third-order tidal potential dominantly modifies the values of ζ_{crit} and μ_{crit} . The numerical results show that the following relations approximately hold:

$$\zeta_{\text{crit}} \approx \zeta_{\text{crit:2nd}} \left(1 - C_1 \frac{R_0}{r} \right), \quad (185)$$

$$\mu_{\text{crit}} \approx \mu_{\text{crit:2nd}} \left(1 + C_2 \frac{R_0}{r} \right), \quad (186)$$

Here, the coefficients of the correction factors C_1 and C_2 are ≈ 0.95 and ≈ 0.80 irrespective of the value of a for $n = 1$. The error is within ~ 0.05 for both coefficients. For $M/r \gtrsim 0.1$, the fourth-order tidal potential becomes important. However, Eqs. (185) and (186) approximately hold even for $r \gtrsim 6M$. For $r \lesssim 6M$, the correction factors in these fitting formulae give overestimated values.

To clarify the importance of the higher-order terms of R_0/r in the tidal potential, in Fig. 3, we show ζ_{crit} and μ_{crit} as functions of r/M (a) for $n = 1$, $a = 0$, and $R_0 = M$, and (b) for $n = 1$, $a = 0.9M$, and $R_0 = M$ with the second-, third-, and fourth-order tidal potentials (dotted, dashed, and solid curves, respectively). With the higher-order tidal potential, the value of ζ_{crit} decreases. Namely, the minimum allowed value of ρ_c increases. This also illustrates that in the second-order approximations, the tidal force is underestimated. For $r/M (= r/R_0) = 6$ (10), the values of ζ_{crit} in the third- and fourth-order approximations are about 13 (8) and 15 (10)% smaller than that in the second-order one. This shows that the standard tidal approximation taken up to the second-order term provides a result with the error of $\sim 10(R_0/M)\%$ for close orbits with $R_0/r \gtrsim 0.1$. However, the convergence appears to be very good if the third- and fourth-order terms are included for $R_0 \lesssim M$. In other words, the fourth-order term plays a quantitatively minor role. All these results agree qualitative with a Newtonian analysis [18].

n	$\zeta_{\text{crit:2nd}}(\text{ISCO})$	$\mu_{\text{crit:2nd}}(\text{ISCO})$	$\zeta_{\text{crit}}(r \rightarrow \infty)$	$\mu_{\text{crit}}(r \rightarrow \infty)$	$M_c(M_\odot)$	C_1	C_2
0	0.0664	20.1	0.0901	14.8	4.54	—	—
0.5	0.0480	19.4	0.0651	14.5	4.45	0.7	0
1.0	0.0303	14.9	0.0411	11.1	3.90	0.95	0.80
1.5	0.0171	13.7	0.0232	10.1	3.74	0.97	0.97

TABLE II. Values of $\zeta_{\text{crit:2nd}}$, $\mu_{\text{crit:2nd}}$, M_c , C_1 , and C_2 for each value of n . The values for $n = 0$ were determined by Fishbone [13]. $\zeta_{\text{crit:2nd}}$ and $\mu_{\text{crit:2nd}}$ do not depend on the value of a , and C_1 and C_2 depend very weakly on it. The value of M_c shown here is that for $a = 0$ and $r = r_{\text{ISCO}} = 6M$, and for $a \neq 0$, $M_c(a) = M_c(a = 0)(6M/r_{\text{ISCO}})^{3/2}$. For the values of C_1 and C_2 , the numerical error is within 5% for $n = 1$ and 1.5, and $\sim 10\%$ for $n = 0.5$.

In Fig. 4(a), we show ζ_{crit} and μ_{crit} as functions of r/M for $n = 1$, $R_0 = M$, and $a/M = 0.9, 0.8, 0.3, 0, -0.3$, and -1 in the fourth-order tidal approximation. For comparison, the results in the second-order approximation are shown in Fig. 4(b). These figures clarify effects of the black hole spin on the Roche limit. For each curve of a given value of a , the minimum value of r is equal to r_{ISCO} . In the second-order tidal approximation, the values of ζ_{crit} and μ_{crit} at the ISCO are independent of a [13] and are about 0.0303 and 14.9, respectively (cf. Table II). In the third- and fourth-order approximations, on the other hand, these values depend slightly on the value of a . As mentioned before, the value of ζ_{crit} (μ_{crit}) in the fourth-order tidal approximation is smaller (larger) than that of $\zeta_{\text{crit:2nd}}$ ($\mu_{\text{crit:2nd}}$). The magnitude of the difference between ζ_{crit} and $\zeta_{\text{crit:2nd}}$ is slightly smaller for a large value of $a \gtrsim 0.9M$ and $a < 0$. The effects of the third- and fourth-order terms in the tidal potential are strongest for $0.3 \lesssim a/M \lesssim 0.8$.

In Figs. 5(a)–(d), the density contour curves in the equatorial plane (\tilde{x}^1 – \tilde{x}^3 plane) at the Roche limit are displayed. Figures 5(a)–(c) are those in the fourth-, third-, and second-order tidal approximations for $r = 6M$, $R_0 = M$, $a = 0$, and $n = 1$, and Fig. 5(d) is in the fourth-order approximation for $r = 2.4M$, $R_0 = M$, $a = 0.9M$, and $n = 1$. In the second-order approximation, the density is symmetric with respect to the $\tilde{x}^1 = 0$ plane, and hence, the asymmetry is induced by the third-order term. At the tidal disruption, $x_s \equiv pq_s \approx 1.6, 1.55$, and $1.5R_0$ in the second-, third-, and fourth-order approximations. On the other hand, the length of the minor axes is $\sim R_0$ independent of the order of the approximation. Thus, in the higher-order approximations, the ellipticity at the Roche limit is slightly smaller. Comparing Figs. 5(a) and (d), it is found that the density configurations near ISCOs for different values of a are very similar irrespective of r .

To clarify the dependence of the Roche limit on the equations of state, we show ζ_{crit} and μ_{crit} for $n = 0.5, 1$, and 1.5 and (a) for $a = 0$ and (b) for $a = 0.9M$ in Fig. 6. The solid and dotted curves for each value of n denote the results in the fourth-order tidal approximation with $R_0 = M$ and in the second-order tidal approximation, respectively. Recall that for $\zeta > \zeta_{\text{crit}}$ or $\mu < \mu_{\text{crit}}$, a star is stable against tidal disruption. This implies that for given values of *mass and radius* ($R_0 \lesssim M$), a star with *softer* equations of state is stronger against tidal disruption than that with the stiffer one. On the other hand, ζ_{crit} is smaller for softer equations of state. This implies that for given values of *central density and radius* ($R_0 \lesssim M$), a star with *stiffer* equations of state is stronger against tidal disruption[‡].

From the analysis of $\zeta_{\text{crit}}/\zeta_{\text{crit:2nd}} - 1$ and $\mu_{\text{crit}}/\mu_{\text{crit:2nd}} - 1$ as functions of M/r , the coefficients C_1 and C_2 are computed for $a = 0$ and $0.9M$. We find that they depend very weakly on a and $C_1 \sim 0.7$ and $C_2 \sim 0$ for $n = 0.5$, and $C_1 \approx 0.97$ and $C_2 \approx 0.97$ for $n = 1.5$. For $n = 0.5$, C_1 and C_2 are not determined very accurately, and hence, the error would be $\sim \pm 0.1$. This is because for very stiff equations of state, the density steeply decreases near the stellar surface and it is not easy to accurately apply the condition for determining the Roche limit (cf. Eq. (184)). Nevertheless, C_1 and C_2 for $n = 0.5$ are much smaller than those for $n = 1$ and 1.5 , and therefore, we can conclude that C_1 and C_2 are larger for softer equations of state. This implies that the third- and fourth-order terms in the tidal potential play a more important role in softer equations of state. For $n = 0.5$, C_2 is approximately zero within the numerical error. This can be explained as follows. The central density at the Roche limit in the fourth-order approximation is always larger than that in the second-order one. On the other hand, the volume of a star at the Roche limit in the fourth-order approximation is smaller than in the second-order one. These two effects seem to approximately cancel for $n = 0.5$.

Computations were also performed including the gravitomagnetic terms associated with A_i for $n = 1$, $R_0/M = 0.5, 1$, and $a/M = 0, 0.9$. In Fig. 7, we display ζ_{crit} and μ_{crit} as functions of r/M . This figure shows that the gravitomagnetic terms decrease ζ_{crit} and increase μ_{crit} for a given value of r , respectively. This implies that the gravitomagnetic tidal force reduces the magnitude of the tidal force. This result is reasonable since the gravitomagnetic force in the Fermi normal coordinate is mainly associated with the coupling between the star's spin and orbital motion, and the spin-orbit coupling force has a repulsive nature in the case that their axes are parallel [30]. The order of magnitude of this term is smaller by the order of r^{-2} as described in the end of Sec. IV A. Thus, it plays an important role only for very small orbital radii $r \lesssim 5M$ as in the fourth-order term of ϕ_{tidal} . The numerical results show that at $r = 6M$, ζ_{crit} and μ_{crit} change only by $\sim 4(R_0/M)\%$ for $a = 0$ and by $\sim 3(R_0/M)\%$ for $a = 0.9M$. However, for rapidly spinning black holes, this term can significantly modify the Roche limit near the ISCOs. Indeed, for $a = 0.9M$ with $r \sim r_{\text{ISCO}} \approx 2.32M$, their values are changed by 20–30% for $R_0 \approx M$.

[‡]Figure 6 suggests that these statements may not be correct for a very large value of $R_0 \gg M$. However, for such a large value of R_0 , the tidal approximation is not applied, and thus, this point is not clear.

D. Application to neutron star-black hole binaries

Now, we apply the results obtained in the previous subsections to binary systems of a neutron star and a black hole. Using the result for $\mu_{\text{crit}} = \mu_{\text{crit:2nd}}(1 + C_2 R_0/r) = (m/M)_{\text{crit}}(r/R_0)^3$, the condition for the mass of a black hole that can tidally disrupt a neutron star outside the ISCO is derived as

$$M \lesssim M_c(a) \left(\frac{R_0}{10 \text{ km}} \right)^{3/2} \left(\frac{m}{1.4 M_\odot} \right)^{-1/2} \left(1 + C_2 \frac{R_0}{r} \right)^{1/2}, \quad (187)$$

where $M_c(a)$ is a function of a . M_c is estimated for $r = r_{\text{ISCO}}$, and thus, it denotes the maximum mass of a black hole that can tidally disrupt neutron stars of a given set of $m = 1.4 M_\odot$, $R_0 = 10 \text{ km}$, and r_{ISCO}/M . The dependence of M_c on a only results from the dependence of r_{ISCO}/M on a since $\mu_{\text{crit:2nd}}$ at the ISCO is independent of a ($\mu_{\text{crit:2nd}} = 19.4, 14.9$, and 13.7 at the ISCOs for $n = 0.5, 1$, and 1.5 ; cf. Table II).

For $a = 0$, $M_c(a = 0) \approx 4.45 M_\odot, 3.90 M_\odot$, and $3.74 M_\odot$ for $n = 0.5, 1$, and 1.5 , respectively. Note that $M_c(a = 0) \approx 4.54 M_\odot$ and $\mu_{\text{crit:2nd}} = 20.1$ at ISCOs for $n = 0$ [13, 17], and thus, they are close to the values for $n = 0.5$. $M_c(a)$ for $a \neq 0$ can be computed by $M_c(a = 0)(6M/r_{\text{ISCO}})^{3/2}$. For a rapidly rotating black hole with $a = 0.99M$ ($0.9M$), $r_{\text{ISCO}}/M \approx 1.4545$ (2.3209), and hence, $M_c \approx 37.3 M_\odot, 32.7 M_\odot$, and $31.3 M_\odot$ ($18.5 M_\odot, 16.2 M_\odot$, and $15.5 M_\odot$) for $n = 0.5, 1$, and 1.5 , respectively. Thus, for the large value of $a/M = 0.9$ – 1 , neutron stars of $R_0 \approx 10 \text{ km}$ are tidally disrupted for a wide mass range of the black hole with $M \lesssim 15$ – $40 M_\odot$. If the typical radius of neutron stars is $R_0 = 15 \text{ km}$, the value of M_c increases by a factor of ≈ 1.84 , and M_c becomes ≈ 30 – $75 M_\odot$ for $a/M = 0.9$ – 1 .

In the second-order tidal approximation, M_c for given values of R_0 and m is smaller for the larger value of n . It is interesting to point out that difference between M_c for $n = 0.5$ and for $n = 1$ is fairly large $\sim 14\%$ although the differences for $n = 1$ and $n = 1.5$ and for $n = 0$ and $n = 0.5$ are only $\sim 4\%$ and $\sim 2\%$, respectively. This suggests that the critical mass ratio Q_{crit} for orbits close to the ISCO depends sensitively on the equations of state in a stiff region of $n = 0.5$ – 1 .

For $n = 1$ and 1.5 , the higher-order terms in the tidal potential increases the critical mass for the tidal disruption. For parameters $M = 4.5 M_\odot$ and $R_0 = 10 \text{ km}$, we obtain $R_0 \approx 1.5M$. In this case, the critical mass with $a = 0$ and $r_{\text{ISCO}} = 6M$ increases by a factor of $\approx 1 + C_2/8$. For $M = 15 M_\odot$ and $R_0 = 10 \text{ km}$, $R_0 \approx 4M/9$. In this case, the critical mass with $a = 0.9M$ and $r_{\text{ISCO}} \approx 2.32M$ increases by a factor of $\approx 1 + C_2/10$. Thus, the critical mass for orbits close to the ISCO increases by $\sim 5\%$ beyond the value of M_c for $n = 1$ and 1.5 due to the effect of the higher-order tidal potential, and hence, the dependence of the critical mass on n would be weaker in reality. Nevertheless, the critical mass near the ISCO still depends fairly strongly on n for $n = 0.5$ – 1 which are plausible polytropic indices for neutron stars [29]. In contrast, ζ_{crit} is smaller for softer equations of state, and the higher-order terms in the tidal potential make this feature stronger.

To clarify its dependence on the orbital radius, in Fig. 8, we display the critical mass of a black hole as a function of r/M . Here, the critical mass in the fourth-order approximation is defined by

$$M_{\text{crit}} = \mu_{\text{crit}}^{1/2} R_0^{3/2} m^{-1/2} \left(\frac{r}{M} \right)^{-3/2}. \quad (188)$$

For $M < M_{\text{crit}}$ at a given orbital radius r/M , the neutron star is tidally disrupted. In Fig. 8, we show M_{crit} for $a = 0$ and $0.9M$, for $R_0 = 10$ and 15 km , and for $n = 0.5, 1$, and 1.5 . It is found that if we assume that the mass of black holes is larger than $3 M_\odot$, the tidal disruption can happen only for close orbits with $r/M \lesssim 7$ for $R_0 = 10 \text{ km}$ and for $r/M \lesssim 10$ for $R_0 = 15 \text{ km}$. Based on an observational results for black hole binaries in our galaxy and in the LMC, typical mass of black holes is in the range between 6 and $8 M_\odot$ [33]. This suggests that the tidal disruption of neutron stars may happen frequently only if (i) the radius of neutron stars is fairly large as $\sim 15 \text{ km}$ or (ii) the typical spin parameter of black holes is fairly large as $a/M \gtrsim 0.6$.

As mentioned above, the values of M_{crit} are very close each other for $n = 1$ and 1.5 irrespective of the orbital radius r/M , and difference in the value of M_{crit} for $n = 0.5$ and 1 is remarkable for $r \sim r_{\text{ISCO}}$. It is interesting to note that the value of M_{crit} depends very weakly on the equations of state for orbits not very close to the ISCO (or in other words for $M_{\text{crit}} \lesssim 4 M_\odot$). The reason is that with increasing r/M , the value of M_{crit} steeply decreases as $M_{\text{crit}}/R_0 \propto (M/r)^{3/2}$, and hence, for a given value of R_0 , the importance of the correction due to the higher-order terms associated with the term $R_0/r = (R_0/M)(M/r)$ in determining M_{crit} is enhanced for $n = 1$ and 1.5 [§]. Nevertheless, M_{crit} for small values

[§] The tidal approximation cannot be used for $M_{\text{crit}} \lesssim 2 M_\odot$ because M_{crit} and r should be much larger than m and R_0 , respectively. Thus, one should focus only on the results for $M \gtrsim M_{\text{crit}}$ in Fig. 8.

of $r/M \lesssim 5$ (or for large black hole mass with $M \gtrsim 4M_\odot$) still depends on the equations of state. This suggests that by determining the tidal disruption limit of binaries of a neutron star and a massive and rapidly spinning black hole in an observation, the equations of state of neutron stars may be constrained.

An observation of binaries composed of a stellar-mass black hole and a neutron star will be possible in the near future using laser interferometric gravitational wave detectors such as LIGO [31]. For the orbital separation $r \gtrsim 10M$, the binary adiabatically evolves due to emission of gravitational waves. In such inspiral phase, the masses of the black hole and the neutron star as well as the black hole spin will be determined from the chirp signal of gravitational waves by using matched filtering techniques [32]. If the mass of the black hole is smaller than the maximum value of M_{crit} , the tidal disruption of the neutron star will happen near an ISCO. It is reasonable to expect that the chirp signal of gravitational waves quickly shutdowns at the tidal disruption. This suggests that from the signal of gravitational waves, the radius and the orbital frequency at the tidal disruption may be identified. With increasing observational samples, M_{crit} (or Q_{crit}) may be determined. If that becomes possible, the equations of state of neutron stars will be constrained.

Unfortunately, the present formulation is not yet appropriate for an accurate determination of the values of M_{crit} and Q_{crit} for a binary of a neutron star and a black hole, since m and R_0 are not much smaller than M and r . Although it is reasonable to expect that dependence of M_{crit} and Q_{crit} on the equations of state is qualitatively unchanged even in a more accurate computation, the values would be systematically modified by 10–20% (see Appendix A). Thus, M_{crit} and Q_{crit} should be determined more accurately in terms of fully general relativistic computations in the future.

VI. SUMMARY AND DISCUSSION

As an extension of previous works by Fishbone [13] and Marck [15], we have derived the tidal potential induced by a black hole up to the fourth order in R/r in the Fermi normal coordinate system using the method developed by Manasse and Misner [19]. The new tidal potential is incorporated into the Newtonian equations of motion for a star orbiting the black hole. Using the new formulation, we determined the tidal disruption limit (Roche limit) for corotating Newtonian stars in equatorial circular orbits around a black hole. It is found that the third- and fourth-order terms in the tidal potential always amplify the tidal force and modify the Roche limit for close orbits. In particular, the third-order term plays a quantitatively important role for orbits with $R/r \gtrsim 0.1$. To this time, tidal problems for a star orbiting a black hole have been widely studied taking into account only the second-order terms of the black hole tidal field (e.g., [13,9,16,17]). The present results illustrate that for close orbits with $R/r \gtrsim 0.1$, the second-order approximation might not provide quantitatively accurate results.

For a specific illustration of the importance of the higher-order terms in the tidal potential as well as the dependence of the Roche limit on the equations of state of the star, numerical computations are performed for plausible parameters of binaries of a black hole and a neutron star. Since neutron stars are general relativistic objects and the mass ratio Q between two stars are not very small, the present framework might not be yet appropriate for such studies. However, it is still possible to extract many qualitative features on the tidal disruption limit. The following is the summary of the results: (i) general relativistic corrections amplify the tidal potential with the decrease of the orbital separation irrespective of the order of the tidal approximation; (ii) as found by Fishbone [13], in the second-order tidal approximation, the minimum value of ζ_{crit} and the maximum value of μ_{crit} are independent of a . In the third- and fourth-order approximations, they depend on a ; (iii) because of the third- and fourth-order terms in the tidal potential, the critical mass ratio Q_{crit} for the tidal disruption is changed by ~ 10 –15% for close orbits near ISCOs with $R_0 \sim M$; (iv) with the increase of the value of spin parameter a , the magnitude of the tidal potential decreases for a given value of r/M , and as a result, ζ_{crit} increases and μ_{crit} decreases. This property is independent of the order of the tidal approximation; (v) for given values of central density and stellar radius ($R_0 \lesssim M$), a neutron star with stiffer equations of state is stronger against tidal disruption. On the other hand, for given values of stellar mass and radius ($R_0 \lesssim M$), a neutron star with softer equations of state is stronger against tidal disruption. The maximum value of μ_{crit} depends sensitively on stiffness of the equations of state for $n = 0.5$ –1.

As mentioned above, the present formulation is not yet appropriate for an accurate determination of the tidal disruption limit of a neutron star by stellar-mass black holes, since the effects of mass, spin, and multipole moments of the neutron star to the orbital motion [34,35] as well as its general relativistic self-gravity are neglected in the analysis. In Appendix A, we estimate the order of magnitude of the error associated with such neglected effects. To more accurately determine the tidal disruption limit, fully general relativistic computation is obviously necessary. We expect that our result presented in this paper could be a guideline for the future computation. In particular, we note that for the case that the mass and radius of a neutron star are much smaller than the black hole mass and orbital radius, respectively, the present formulation provides an accurate result for the Roche limit. The fully general relativistic results computed in the future should be compared with our numerical results to check the accuracy.

So far, we have focused on binaries of a black hole and a neutron star. The results with $n = 1.5$ may be used for determining the Roche limit of a white dwarf near the ISCO of a massive black hole. For typical values of mass $\sim 0.7M_\odot$ and radius $\sim 10^4$ km of a white dwarf with $n \approx 1.5$ [29,36], Eq. (187) is written as

$$M \lesssim 1.67 \times 10^5 M_\odot \left(\frac{R_0}{10^4 \text{ km}} \right)^{3/2} \left(\frac{m}{0.7M_\odot} \right)^{-1/2} \left(\frac{r}{6M} \right)^{-3/2} \left(\frac{\mu_{\text{crit}}}{13.7} \right)^{1/2}. \quad (189)$$

In this case, $R_0/r \ll 1$, and therefore, the third- and fourth-order terms in the tidal potential are not important and can be neglected. Equation (189) implies that an intermediate-mass black hole of $M \sim 10^3 M_\odot$ will tidally disrupt a typical white dwarf in a circular orbit at $r \sim 160M$. To tidally disrupt a typical white dwarf in a circular orbit, a supermassive black hole of $M \sim 10^6 M_\odot$ has to be rapidly rotating with $a \gtrsim 0.95M$ for which $r_{\text{ISCO}} \lesssim 2M$.

White dwarfs orbiting a supermassive black hole in galactic centers are likely to have highly elliptic orbits with $E \approx 1$ or parabolic orbits with $E = 1$ (e.g., [37,38]). Even in this case, the values of M_{crit} , which are determined for the circular orbits with $r \approx r_{\text{ISCO}}$, may be used for determining the upper mass of a black hole, M_{max} , for which a white dwarf with $E \approx 1$ is tidally disrupted. The reason is that the tidal disruption limit will be determined by the tidal force at the periastron radius and thus M_{max} will be determined by the radius of the marginally bound orbits. For highly elliptic or parabolic orbits in general relativity, the marginally bound orbits become the so-called zoom-whirl orbits [39], which have a nearly circular trajectory near the periastron with the orbital radius [29]

$$r = r_{\text{mb}} = 2M - a + 2M\sqrt{1 - a/M}. \quad (190)$$

Therefore, the analysis in assumption of the circular orbits is approximately applicable. Here, the circular orbits with $r = r_{\text{mb}}$ is unstable. Nevertheless, we can estimate the Roche limit by the analysis presented in Sec V mathematically.

The result is that $\mu_{\text{crit:2nd}} \approx 20.7$ for $n = 1.5$ irrespective of value of a . Here, we note that for such circular orbits with $E = 1$ and $r = r_{\text{mb}}$, $B/r = 1$ independent of a , and so is $\mu_{\text{crit:2nd}}$. Replacing r_{ISCO} to r_{mb} and adopting the new value of $\mu_{\text{crit:2nd}}$, we can approximately estimate M_{max} of the black hole for the tidal disruption of a white dwarf in highly elliptic or parabolic orbits as

$$M_{\text{max}} \approx 3.77 \times 10^5 M_\odot \left(\frac{R_0}{10^4 \text{ km}} \right)^{3/2} \left(\frac{m}{0.7M_\odot} \right)^{-1/2} \left(\frac{r_{\text{mb}}}{4M} \right)^{-3/2}. \quad (191)$$

Therefore, a black hole of $M \lesssim 3.8 \times 10^5 M_\odot$ and $a = 0$ ($M \lesssim 3 \times 10^6 M_\odot$ and $a \approx M$) can tidally disrupt white dwarfs of $m \approx 0.7M_\odot$ and $R_0 \approx 10^4$ km.

In this paper, we have only studied the tidal disruption limit for a star in equatorial circular orbits. The formulation derived in this paper can be used for the hydrodynamic tidal problem of an ordinary star or a white dwarf in parabolic orbits around a supermassive black hole [16]. In Appendix B, we write the tidal potential for a parabolic orbit in the equatorial plane, which may be used for an extension of the works presented in [16]. To confirm the prediction (191) for the tidal disruption of white dwarfs by a supermassive black hole, we plan to perform numerical simulations.

ACKNOWLEDGMENTS

We are grateful Kip Thorne for pointing out the importance of higher-order terms in the tidal potentials. His suggestion motivates this work. Algebraic manipulations in Secs. III, IV, and Appendix B were performed by Mathematica. This work was supported by Japanese Monbukagaku-Sho Grant Nos. 14047207, 15037204, 15740142, and 16029202. YM was supported by the NASA Center for Gravitational Wave Astronomy at University of Texas at Brownsville (NAG5-13396), and grant NSF-PHY-0140326.

APPENDIX A: ORDER OF MAGNITUDE OF THE ERROR

In the analysis for the tidal disruption limit of a star by black holes in terms of the present tidal approximation, we neglect the effects associated with the mass, spin, and multipole moments of the companion star to its orbital motion. Here, we estimate the order of magnitude of the error due to neglecting these effects.

Neglecting the mass of the star results in the error of the orbital angular velocity by a factor of m/M . This error is included in the centrifugal force associated with the corotating velocity field (cf. Eq. (168)). Since the order of magnitude of the centrifugal force is nearly identical with the tidal force, the values of ζ_{crit} and μ_{crit} which characterize the tidal disruption limit would be modified by a factor $\lesssim m/2M \sim 1\text{--}20\%$ for $m = 1.4M_\odot$ and $M = M_{\text{crit}} \sim 4\text{--}50M_\odot$.

An equation of motion for an extended body was considered in [35] ignoring the self-gravity of the body. If we take into account the spin and quadrupole moment of the body, we have the equations of motion

$$\frac{D}{ds}p_\alpha = \frac{1}{2}v^\beta S^{\gamma\delta} R_{\alpha\beta\gamma\delta} + \frac{1}{6}J^{\beta\gamma\delta\epsilon}\nabla_\alpha R_{\beta\gamma\delta\epsilon}, \quad (\text{A1})$$

where p^α is the momentum vector, s an affine parameter (see Eq.171 in [35]), $S^{\alpha\beta}$ the spin tensor, and $J^{\alpha\beta\gamma\delta}$ the quadrupole mass distribution of the extended body. In the post-Newtonian approximation, two terms in the right-hand side of Eq. (A1) are estimated as

$$\delta F_\alpha^s \equiv \frac{1}{2}v^\beta S^{\gamma\delta} R_{\alpha\beta\gamma\delta} \sim \frac{mMR^2\Omega^2}{r^2} \sim \frac{mM^2R^2}{r^5}, \quad (\text{A2})$$

$$\delta F_\alpha^q \equiv J^{\beta\gamma\delta\epsilon}\nabla_\alpha R_{\beta\gamma\delta\epsilon} \sim \frac{mM^2R^4}{r^7}. \quad (\text{A3})$$

where we assume that the orbital angular velocity Ω is equal to the spin angular velocity observed by a comoving frame, and that the quadrupole moment is induced by the black hole tidal field. The ratio of these terms to the Newtonian force is

$$\frac{\delta|F_\alpha^s|}{Mm/r^2} \sim \frac{MR^2}{r^3}, \quad (\text{A4})$$

$$\frac{\delta|F_\alpha^q|}{Mm/r^2} \sim \frac{MR^4}{r^5}. \quad (\text{A5})$$

Thus, these corrections modify the orbital angular velocity by a factor of $\sim MR^2/r^3$ and $\sim MR^4/r^5$, respectively. They are likely to be much smaller than m/M for neutron star binaries. We note that for the irrotational velocity field, the correction due to the spin is approximately zero.

With the modification of the orbital motion, the location of the ISCO will be modified. By this effect, $\zeta_{\text{crit:min}}$ and $\mu_{\text{crit:max}}$ will be also modified.

APPENDIX B: TIDAL TENSORS FOR EQUATORIAL PARABOLIC ORBITS

In Sec. IV, we derive the formulation of the tidal problem for a star in equatorial circular orbits. Another interesting case is a parabolic encounter of an ordinary star or a white dwarf with a supermassive black hole. Here, we write the tidal potential for equatorial parabolic orbits.

For equatorial parabolic orbits with $E = 1$ and $L > L_{\text{crit}}$ where L_{crit} is a critical value which depends on a and $L_{\text{crit}} = 4M$ for $a = 0$, the first integrals of the geodesic equations are written as

$$u^t = \frac{1}{\Delta r^2} \left[(r^2 + a^2)r^2 - 2Mar\ell \right], \quad (\text{B1})$$

$$u^r = \pm V_1, \quad (\text{B2})$$

$$u^\varphi = \frac{-2M\ell + Lr}{\Delta r}, \quad (\text{B3})$$

and $u^\theta = 0$. Here,

$$V_1 \equiv \sqrt{\left(1 - \frac{a\ell}{r^2}\right)^2 - \frac{\Delta}{r^2}V_2^2}, \quad V_2 \equiv \sqrt{1 + \frac{\ell^2}{r^2}}, \quad (\text{B4})$$

and $\ell \equiv L - a$. Then, the nonzero components of the tidal tensor in the tilde frame are

$$\tilde{C}_{11} = \frac{M}{r^3} \left(1 - 3\frac{r^2 + \ell^2}{r^2} \right), \quad (\text{B5})$$

$$\tilde{C}_{22} = \frac{M}{r^3} \left(1 + 3\frac{\ell^2}{r^2} \right), \quad (\text{B6})$$

$$\tilde{C}_{33} = \frac{M}{r^3}, \quad (\text{B7})$$

$$\tilde{B}_{131} = \tilde{B}_{311} = -\tilde{B}_{232} = -\tilde{B}_{322} = -\frac{1}{2}\tilde{B}_{113} = \frac{1}{2}\tilde{B}_{223} = -\frac{3M\ell V_2}{2r^4}, \quad (\text{B8})$$

$$\tilde{C}_{111} = \frac{3M}{r^4 V_2} \left[2 + \frac{3\ell^2 - 4a\ell}{r^2} - \frac{5a\ell^3}{r^4} \right], \quad (\text{B9})$$

$$\tilde{C}_{131} = \tilde{C}_{311} = \tilde{C}_{113} = \pm \frac{M\ell V_1}{r^5 V_2} \left[4 + \frac{5\ell^2}{r^2} \right], \quad (\text{B10})$$

$$\tilde{C}_{122} = \tilde{C}_{212} = \tilde{C}_{221} = -\frac{M}{r^4 V_2} \left[3 + \frac{7\ell^2 - 11a\ell}{r^2} - \frac{15a\ell^3}{r^4} \right], \quad (\text{B11})$$

$$\tilde{C}_{133} = \tilde{C}_{313} = \tilde{C}_{331} = -\frac{M}{r^4 V_2} \left[3 + \frac{2\ell^2 - a\ell}{r^2} \right], \quad (\text{B12})$$

$$\tilde{C}_{322} = \tilde{C}_{232} = \tilde{C}_{223} = \mp \frac{M\ell V_1}{r^5 V_2} \left[1 + \frac{5\ell^2}{r^2} \right], \quad (\text{B13})$$

$$\tilde{C}_{333} = \mp \frac{3M\ell V_1}{r^5 V_2}, \quad (\text{B14})$$

$$\tilde{C}_{1111} = \frac{3M}{r^5 V_2^2} \left[-8 + \frac{2M}{r} - \frac{12\ell^2 - 32a\ell + 4a^2}{r^2} + \frac{5M\ell^2}{r^3} + \frac{40a\ell^3 - 35a^2\ell^2}{r^4} + \frac{3\ell^4 M}{r^5} - \frac{35a^2\ell^4}{r^6} \right], \quad (\text{B15})$$

$$\tilde{C}_{1113} = \tilde{C}_{1131} = \tilde{C}_{1311} = \tilde{C}_{3111} = \mp \frac{3M}{2r^6 V_2^2} \left[16\ell - 4a + \frac{20\ell^3 - 35a\ell^2}{r^2} - \frac{35a\ell^4}{r^4} \right] V_1, \quad (\text{B16})$$

$$\begin{aligned} \tilde{C}_{1122} &= \tilde{C}_{1212} = \tilde{C}_{1221} = \tilde{C}_{2112} = \tilde{C}_{2121} = \tilde{C}_{2211} \\ &= -\frac{M}{2r^5 V_2^2} \left[-24 + \frac{11M}{r} - \frac{55\ell^2 - 148a\ell + 31a^2}{r^2} + \frac{28M\ell^2}{r^3} - \frac{5\ell^4 - 200a\ell^3 + 215a^2\ell^2}{r^4} + \frac{17M\ell^4}{r^5} - \frac{210a^2\ell^4}{r^6} \right], \end{aligned} \quad (\text{B17})$$

$$\begin{aligned} \tilde{C}_{1133} &= \tilde{C}_{1313} = \tilde{C}_{1331} = \tilde{C}_{3113} = \tilde{C}_{3131} = \tilde{C}_{3311} \\ &= -\frac{M}{2r^5} \left[-24 + \frac{11M}{r} - \frac{5\ell^2 - 20a\ell + 5a^2}{r^2} + \frac{76M\ell^2}{r^3} - \frac{35\ell^4 + 70a\ell^3 + 35a^2\ell^2}{r^4} + \frac{75M\ell^4}{r^5} \right], \end{aligned} \quad (\text{B18})$$

$$\begin{aligned} \tilde{C}_{1223} &= \tilde{C}_{1232} = \tilde{C}_{1322} = \tilde{C}_{2123} = \tilde{C}_{2132} = \tilde{C}_{3122} = \tilde{C}_{2213} = \tilde{C}_{2312} = \tilde{C}_{3212} = \tilde{C}_{2231} = \tilde{C}_{2321} = \tilde{C}_{3221} \\ &= \pm \frac{M}{2r^6 V_2^2} \left[14\ell - a + \frac{40\ell^3 - 80a\ell^2}{r^2} - \frac{105a\ell^4}{r^4} \right] V_1, \end{aligned} \quad (\text{B19})$$

$$\tilde{C}_{1333} = \tilde{C}_{3133} = \tilde{C}_{3313} = \tilde{C}_{3331} = \pm \frac{3M}{2r^6 V_2^2} \left[14\ell - a + \frac{10\ell^3 - 5a\ell^2}{r^2} \right] V_1, \quad (\text{B20})$$

$$\tilde{C}_{2222} = \frac{3M}{r^5} \left[-3 + \frac{2M}{r} - \frac{5\ell^2 - 20a\ell + 5a^2}{r^2} + \frac{10M\ell^2}{r^3} - \frac{35a^2\ell^2}{r^4} \right], \quad (\text{B21})$$

$$\begin{aligned} \tilde{C}_{2233} &= \tilde{C}_{2332} = \tilde{C}_{3332} = \tilde{C}_{3223} = \tilde{C}_{3232} = \tilde{C}_{3322} \\ &= -\frac{M}{2r^5 V_2^2} \left[-6 + \frac{4M}{r} - \frac{12\ell^2 - 18a\ell + 6a^2}{r^2} + \frac{25M\ell^2}{r^3} - \frac{15\ell^4 + 15a^2\ell^2}{r^4} + \frac{96M\ell^4}{r^5} \right. \\ &\quad \left. - \frac{35\ell^6 + 70a\ell^5 + 35a^2\ell^4}{r^6} + \frac{75M\ell^6}{r^7} \right], \end{aligned} \quad (\text{B22})$$

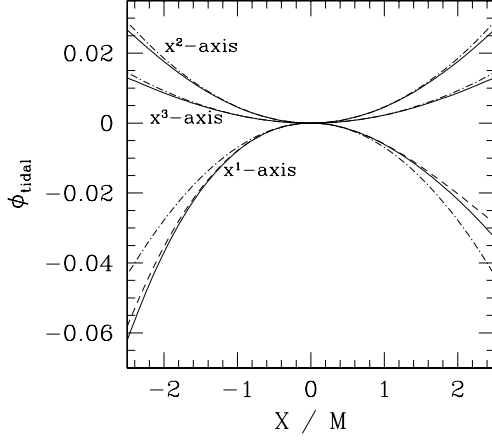
$$\tilde{C}_{3333} = \frac{3M}{r^5 V_2^2} \left[-3 + \frac{2M}{r} - \frac{4\ell^2 + 2a\ell + a^2}{r^2} + \frac{13M\ell^2}{r^3} - \frac{5\ell^4 + 10a\ell^3 + 5a^2\ell^2}{r^4} + \frac{11M\ell^4}{r^5} \right]. \quad (\text{B23})$$

Components in the Fermi normal coordinates are calculated by operating rotational matrices associated with Ψ as in Sec. IV. Here, evolution equation of the rotation angle is written as

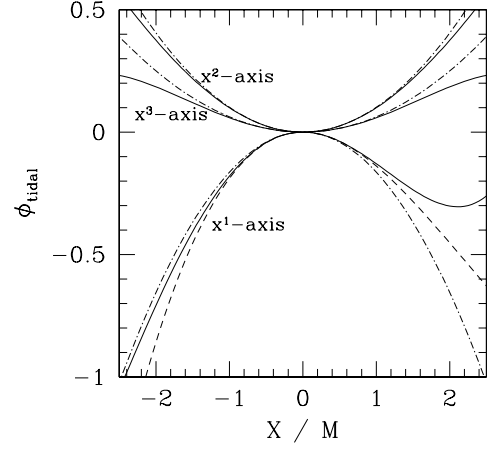
$$\frac{d\Psi}{d\tau} = \frac{L}{r^2 + \ell^2}. \quad (\text{B24})$$

If computations are performed in the tilde frame, Ψ is not necessary for computing the tidal potential. Instead, $d\Psi/d\tau$ and $d^2\Psi/d\tau^2$ appear in computing the inertial forces in the equations of motion.

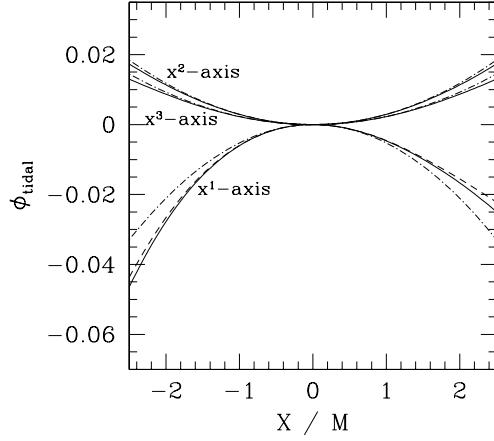
- [1] S. Ayal, M. Livio, and T. Piran, *Astrophys. J.* **545**, 772 (2000).
- [2] T. Bogdanovic, M. Eracleous, S. Mahadevan, S. Sigurdsson, and P. Laguna, *Astrophys. J.* **610**, 707 (2004).
- [3] C. L. Fryer, S. E. Woosley, M. Herant, and M. B. Davies, *Astrophys. J.* **520**, 650 (1999).
- [4] C. Cutler et al., *Phys. Rev. Lett.* **70**, 2984 (1993).
- [5] M. Vallisneri, *Phys. Rev. Lett.* **84**, 3519 (2000).
- [6] C. R. Evans and C. S. Kochanek, *Astrophys. J.* **346**, L13 (1989).
- [7] K. Uryu and Y. Eriguchi, *Mon. Not. R. astr. Soc.* **303**, 329 (1999).
- [8] H.-T. Janka, T. Eberl, M. Ruffert, and C. L. Fryer, *Astrophys. J.* **527**, L39 (1999).
- [9] B. Carter and J.-P. Luminet, *Astron. Astrophys.* **121**, 97 (1983); *Mon. Not. R. astr. Soc.* **212**, 23 (1985).
- [10] A. Khokhlov, I. D. Novikov, and C. J. Pethick, *Astrophys. J.* **418**, 163 (1993); *ibid* **418**, 181 (1993).
- [11] J. A. Marck, A. Lioure, and S. Bonazzola, *Astron. Astrophys.* **306**, 666 (1996).
- [12] P. Laguna, W. A. Miller, W. H. Zurek, and M. B. Davies, *Astrophys. J.* **410**, L83 (1993).
- [13] L. G. Fishbone, *Astrophys. J.* **185**, 43 (1973).
- [14] B. Mashhoon, *Astrophys. J.* **197**, 705 (1975).
- [15] J.-A. Marck, *Proc. R. Soc. Lond. A* **385**, 431 (1983).
- [16] V. P. Frolov, A. M. Khokhlov, I. D. Novikov, and C. J. Pethick, *Astrophys. J.* **432**, 680 (1994); P. Diener, V. P. Frolov, A. M. Khokhlov, I. D. Novikov, and C. J. Pethick, *Astrophys. J.* **479**, 164 (1997).
- [17] M. Shibata, *Prog. Theor. Phys.* **96**, 917 (1996).
- [18] M. Ishii and M. Shibata, *Prog. Theor. Phys.* **112**, 399 (2004).
- [19] F. K. Manasse and C. W. Misner, *J. Math. Phys.* **4**, 735 (1963).
- [20] J. M. Bardeen, W. H. Press, and S. A. Teukolsky, *Astrophys. J.* **178**, 347 (1972).
- [21] M. Miller, gr-qc/0106017.
- [22] T. W. Baumgarte, M. L. Skoge, and S. L. Shapiro, gr-qc/0405077.
- [23] R. M. Wald, *General relativity* (The University of Chicago Press, Chicago and London, 1984).
- [24] S. Chandrasekhar, *The Mathematical Theory of Black Holes*, Oxford Science Publications (Oxford University Press, New York, 1983), chapter 6.
- [25] B. Carter, *Phys. Rev.* **174**, 1559 (1968).
- [26] K. S. Thorne, R. H. Price, and D. A. Macdonald, *The Membrane Paradigm* (Yale University Press, New Haven and London, 1986).
- [27] C. W. Misner, K. S. Thorne, and J. A. Wheeler, *Gravitation* (Freeman, San Francisco, 1973).
- [28] M. Shibata, *Prog. Theor. Phys.* **96**, 317 (1996); *Phys. Rev. D* **55**, 6019 (1997).
- [29] S. L. Shapiro and S. A. Teukolsky, *Black Holes, White Dwarfs, and Neutron Stars*, Wiley Interscience (New York, 1983), chapter 12.
- [30] E.g., L. E. Kidder, C. M. Will, and A. G. Wiseman, *Phys. Rev. D* **47**, R4183 (1993) and references therein.
- [31] C. Cutler and K. S. Thorne, in *Proceedings of the 16th International Conference on General Relativity and Gravitation*, edited by N. T. Bishop and S. D. Maharaj (World Scientific, 2002), p.72.
- [32] C. Cutler and E. E. Flanagan, *Phys. Rev. D* **49**, 2658 (1994).
- [33] J. E. McClintock and R. A. Remillard, in *Compact Stellar X-ray Sources*, edited by W. H. G. Lewin and van der Klis (Cambridge University Press, Cambridge, 2005) to be published (astro-ph/0306213).
- [34] A. Papapetrou, *Proc. R. Soc. London Ser. A* **209**, 248 (1951).
- [35] W. G. Dixon, in *Isolated Gravitating Systems in General Relativity*, edited by J. Ehlers (North-Holland, Amsterdam, 1979), pp. 156.
- [36] V. Weidemann, *Annu. Rev. Astron. Astrophys.* **28**, 103 (1990).
- [37] D. Hils and P. L. Bender, *Astrophys. J. Lett.* **445**, L7 (1995).
- [38] M. Shibata, *Phys. Rev. D* **50**, 6297 (1994).
- [39] K. Glampedakis and D. Kennefick, *Phys. Rev. D* **66**, 044002 (2002).



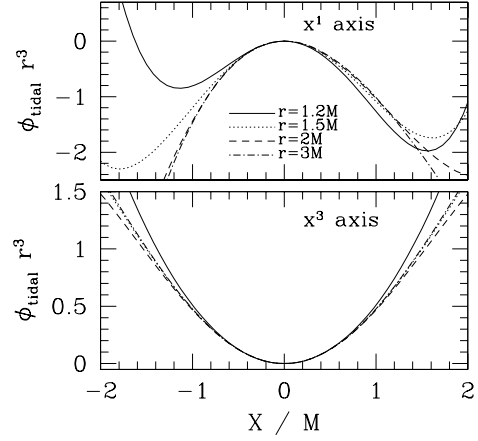
(a)



(b)



(c)



(d)

FIG. 1. The profiles of the tidal potential ϕ_{tidal} along x^1 , x^2 , and x^3 axes (a) for $r = 6M$ and $a = 0$, (b) for $r = 2M$ and $a = M$, (c) for $r = 6M$ and $a = M$, and (d) for $r/M = 1.2, 1.5, 2$, and 3 and $a = M$. The solid, dashed, and dotted-dashed curves in panels (a)–(c) denote ϕ_{tidal} in the fourth-, third-, and second-order approximations, respectively. In panel (d), the tidal potential in the fourth-order approximation along x^1 and x^3 axes are shown. The units of $G = M = 1$ are adopted in these figures.

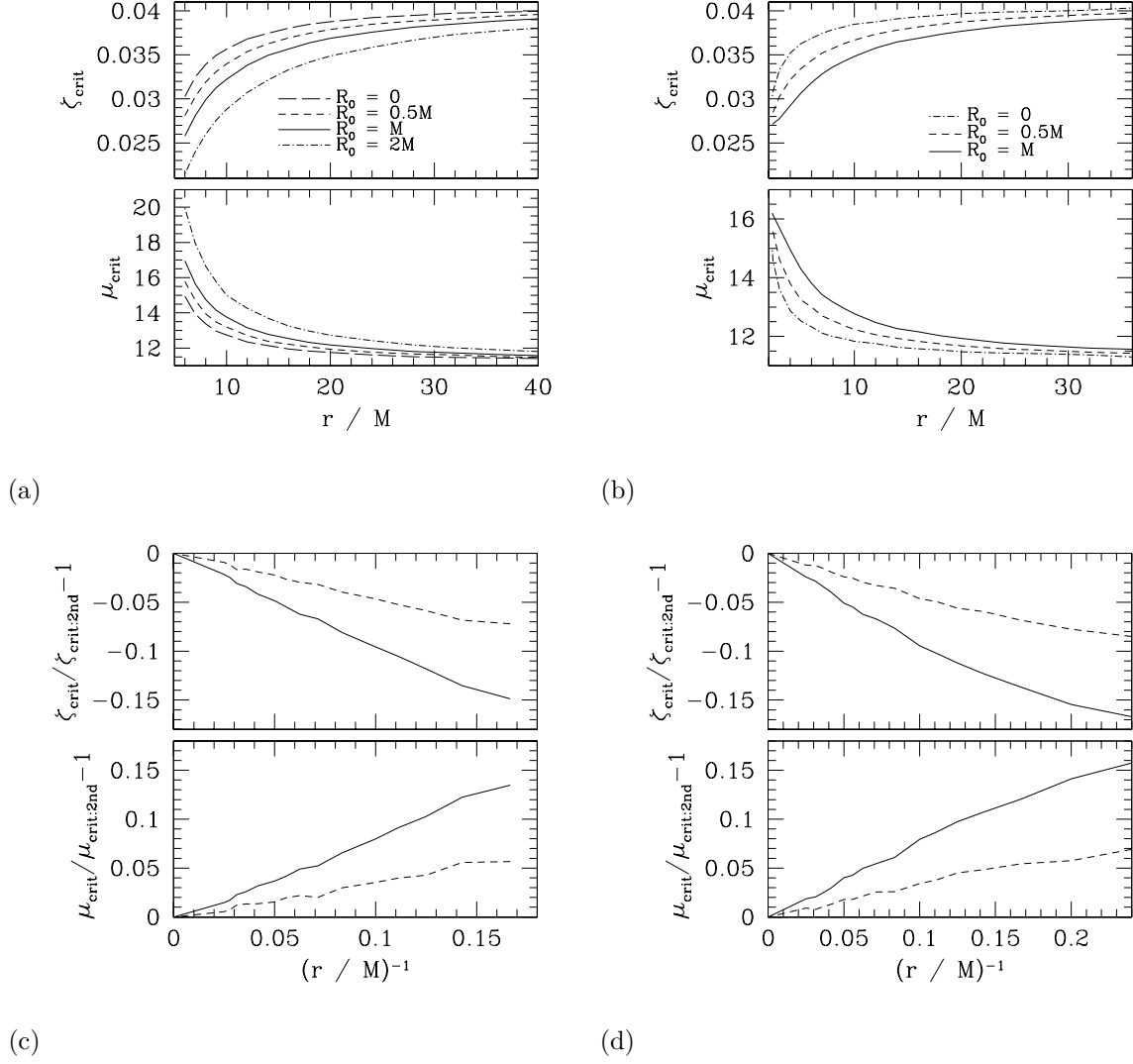


FIG. 2. (a) ζ_{crit} and μ_{crit} as functions of r for $R_0/M = 0, 0.5, 1$, and 2 , and for $a = 0$. (b) the same as (a) but for $R_0/M = 0, 0.5$, and 1 and for $a = 0.9M$. (c) $\zeta_{\text{crit}}/\zeta_{\text{crit:2nd}} - 1$ as a function of M/r for $R_0/M = 0.5$ (dashed curve) and 1 (solid curve), and for $a = 0$. (d) the same as (c) but for $a = 0.9M$. Here, $n = 1$. $\zeta_{\text{crit:2nd}}$ is ζ_{crit} with $R_0 = 0$ and equal to that in the second-order tidal approximation. We note that a star with $\zeta > \zeta_{\text{crit}}$ (or $\mu < \mu_{\text{crit}}$) for a given value of r/M is unstable against tidal disruption.

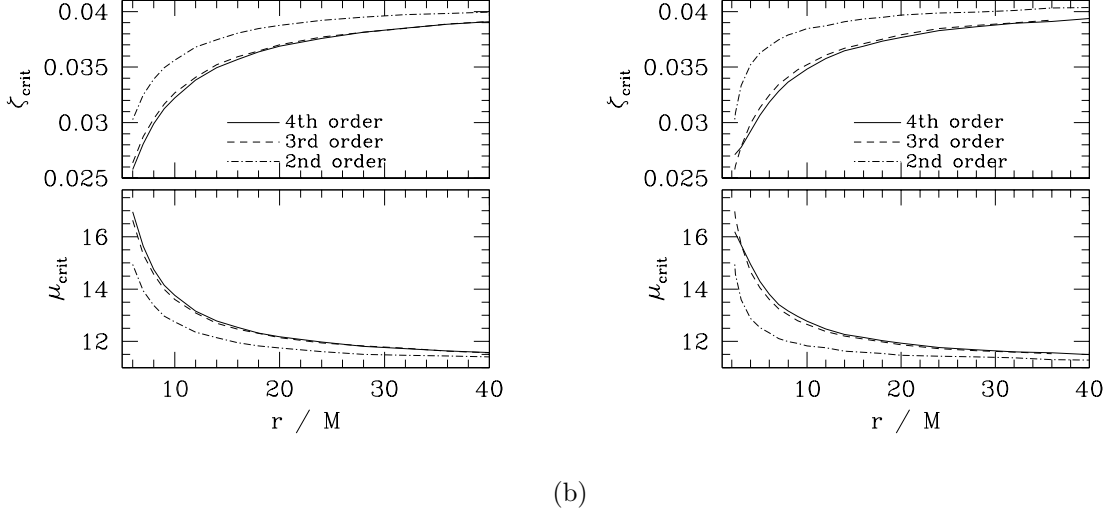


FIG. 3. ζ_{crit} and μ_{crit} as functions of r (a) for $a = 0$ and (b) for $a = 0.9M$. For both cases, $n = 1$ and $R_0 = M$. The solid, dashed, and dotted-dashed curves denote the results in the fourth-, third-, and second-order tidal approximations, respectively.

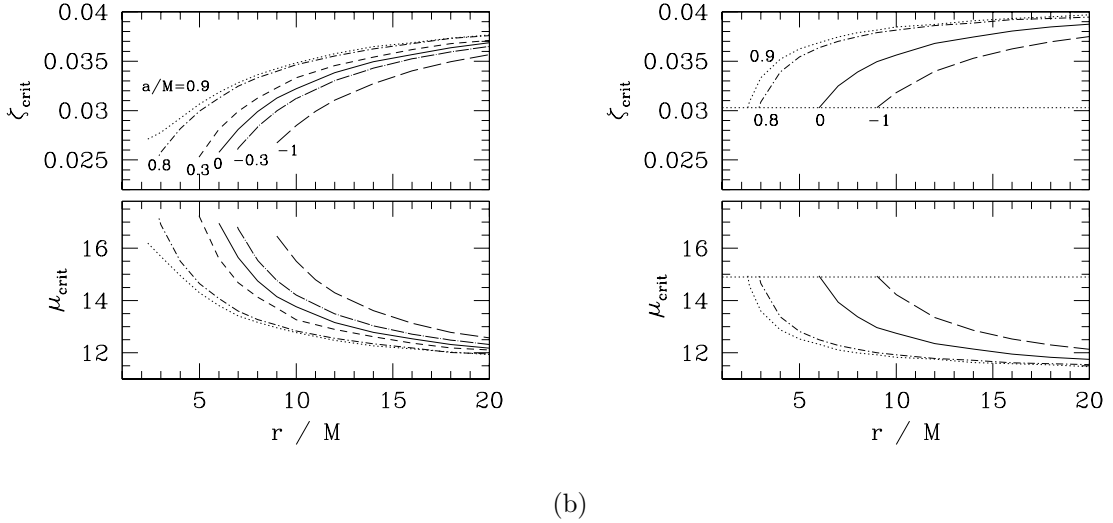


FIG. 4. ζ_{crit} and μ_{crit} as functions of r for $n = 1$ and various values of a/M . (a) The dotted, dotted-dashed, dashed, solid, dotted-long-dashed, and long-dashed curves denote the results in the fourth-order tidal approximation with $R_0 = M$ for $a/M = 0.9, 0.8, 0.3, 0, -0.3,$ and -1 , respectively. (b) The dotted, dotted-dashed, solid, and long-dashed curves denote the results in the second-order tidal approximation for $a/M = 0.9, 0.8, 0,$ and -1 , respectively. Note that in the second-order tidal approximation, ζ_{crit} and μ_{crit} at ISCOs are about 0.0303 and 14.9 irrespective of the value of a (dotted horizontal lines).

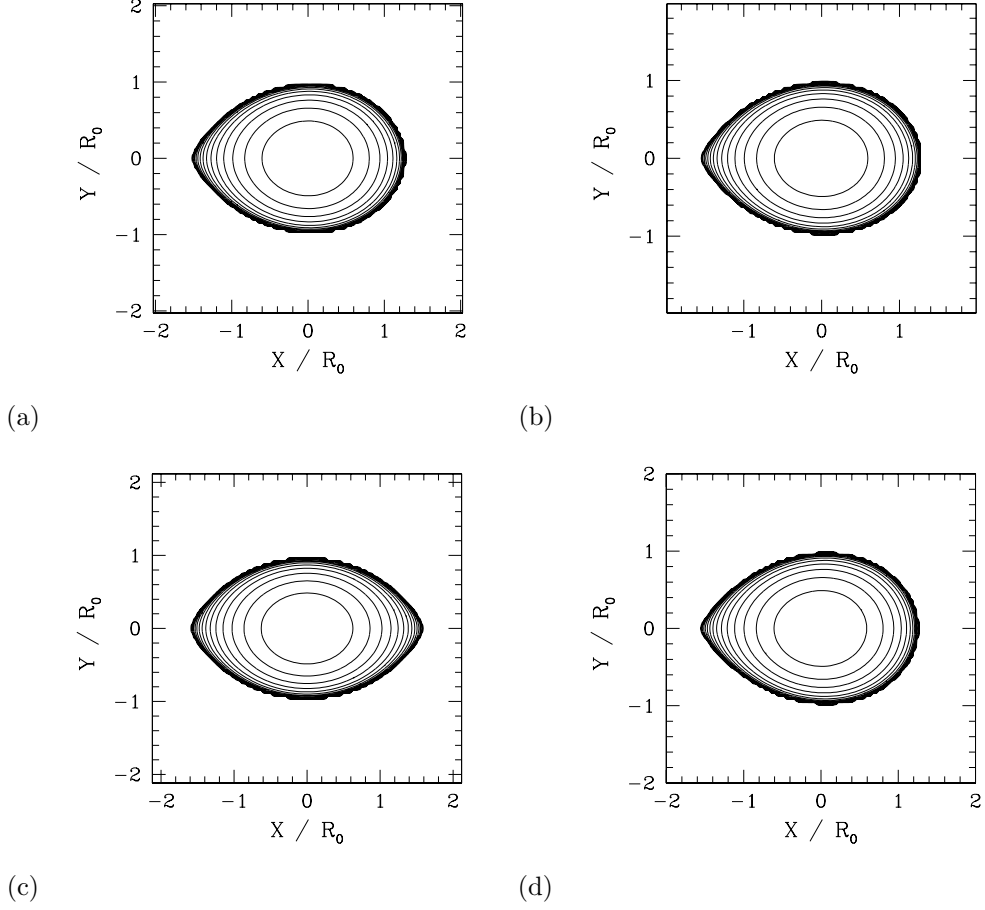


FIG. 5. Density contour curves at Roche limits in the (a) fourth-, (b) third-, and (c) second-order tidal approximations for $r = 6M$, $R_0 = M$, $a = 0$, and $n = 1$. (d) density contour curves at a Roche limit in the fourth-order approximation for $r = 2.4M$, $R_0 = M$, $a = 0.9M$, and $n = 1$. The contour curves are drawn for $\rho/\rho_c = 10^{-0.2j}$ for $j = 0, 1, 2, \dots, 15$. X and Y denote \tilde{x}^1 and \tilde{x}^3 , respectively.

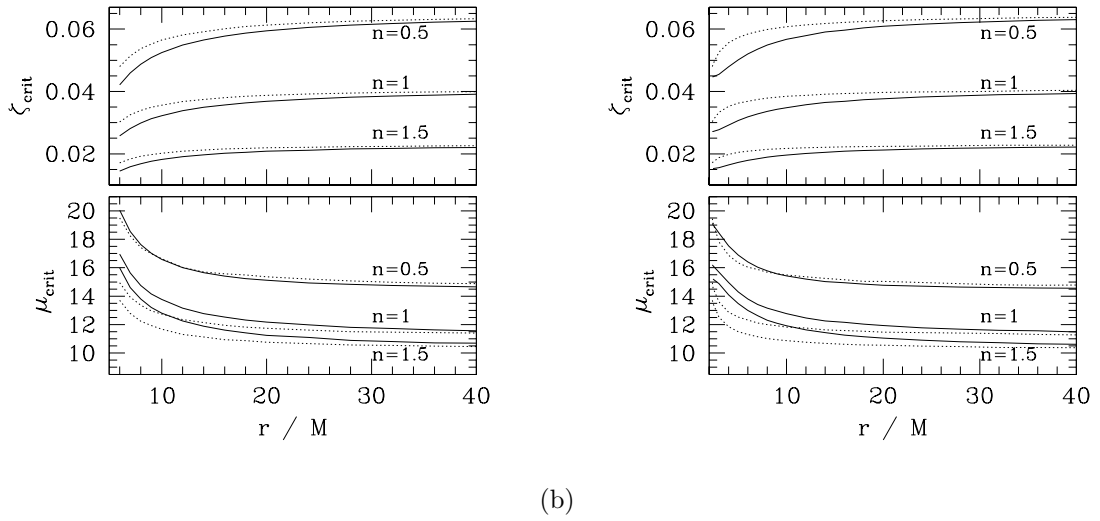


FIG. 6. ζ_{crit} and μ_{crit} as functions of r (a) for $a = 0$ and (b) for $a = 0.9M$. For both figures, the results with $n = 0.5, 1$, and 1.5 are shown. The solid and dotted curves for each value of n denote the results in the fourth-order tidal approximation with $R_0 = M$ and in the second-order tidal approximation, respectively.

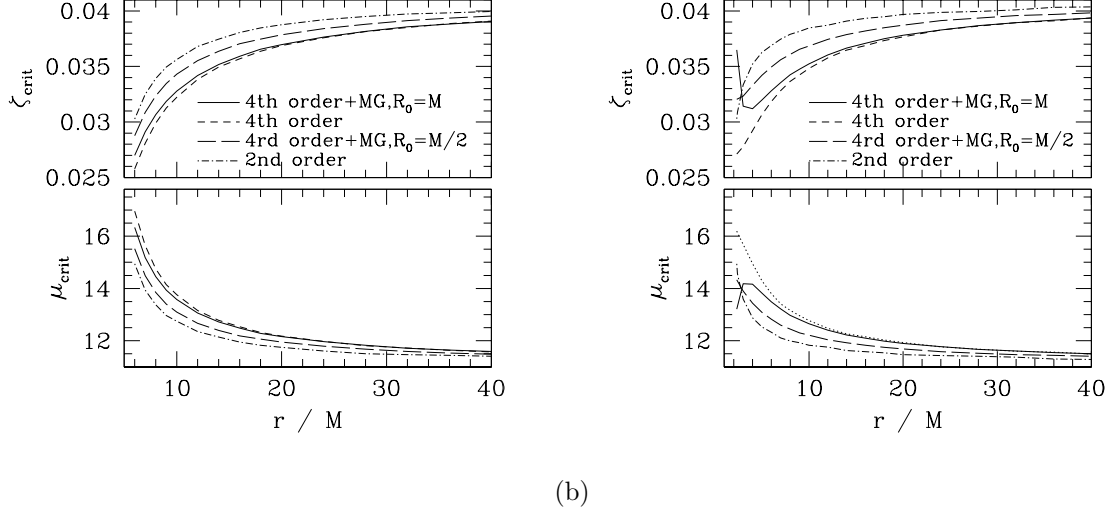


FIG. 7. ζ_{crit} and μ_{crit} as functions of r in the presence of the gravitomagnetic (GM) term (a) for $a = 0$ and (b) for $a = 0.9M$. For both figures, the results with $n = 1$ and with $R_0/M = 0.5$ and 1 are shown. The solid, dashed, long-dashed, and dotted-dashed curves denote the results in the fourth-order tidal approximation with the GM term and for $R_0 = M$, in the fourth-order tidal approximation with no GM term and for $R_0 = M$, and in the fourth-order tidal approximation with the GM term and for $R_0 = 0.5M$, and in the second-order tidal approximation with no GM term, respectively.

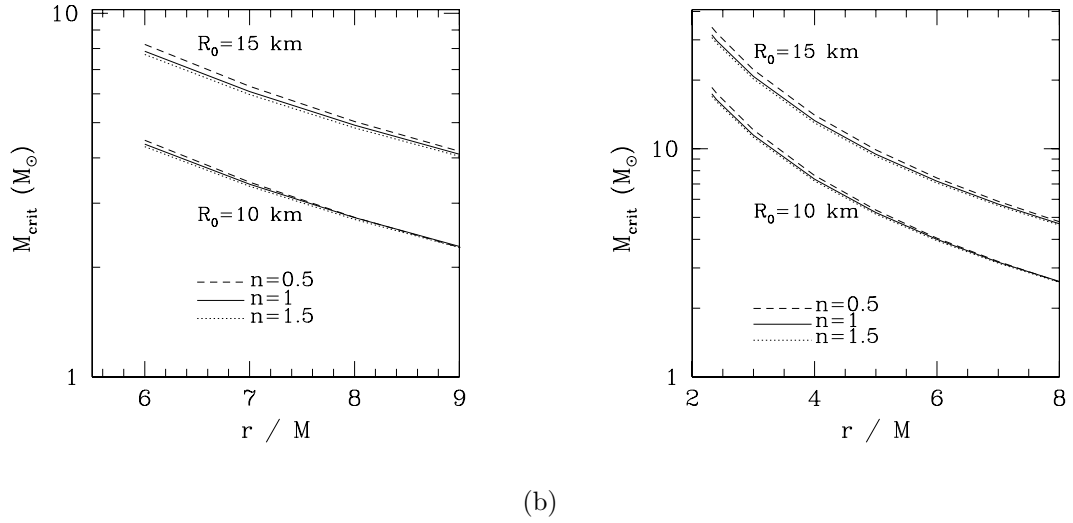


FIG. 8. Critical mass M_{crit} of a black hole for the tidal disruption of a neutron star of mass $1.4M_{\odot}$ and radius $R_0 = 10$ km and 15 km as a function of r/M (a) for $a = 0$ and (b) for $a = 0.9M$. The dashed, solid, and dotted curves denote the results for $n = 0.5, 1$, and 1.5 , respectively. For $M < M_{\text{crit}}$ at a given value of r/M , the neutron star is unstable against tidal disruption.